

Aspects of Lattice QCD calculations of transverse momentum-dependent parton distributions (TMDs)

Michael Engelhardt

New Mexico State University

In collaboration with:

B. Musch, P. Hägler, J. Negele, A. Schäfer
T. Bhattacharya, R. Gupta, B. Yoon
S. Syritsyn, A. Pochinsky, J. R. Green, S. Meinel

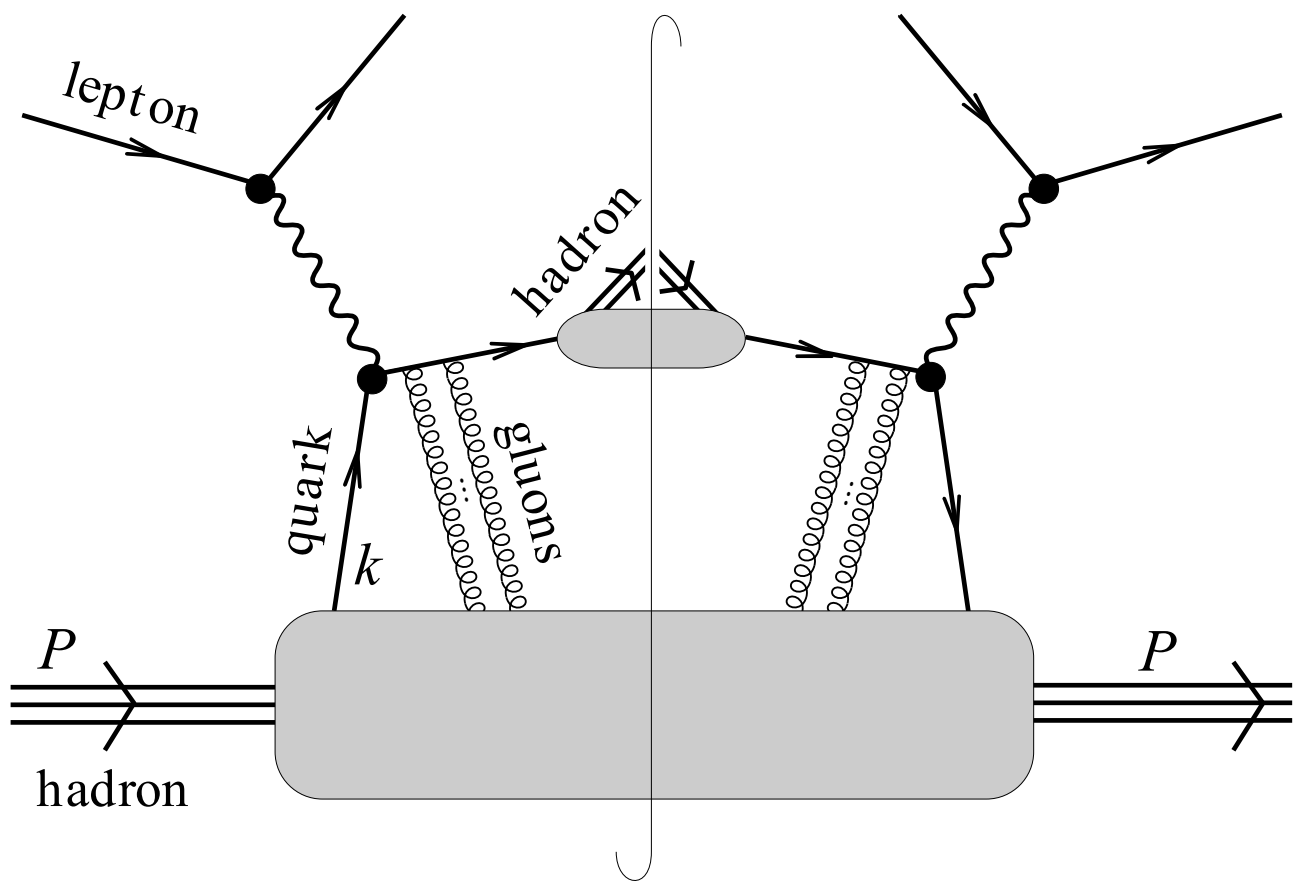
Fundamental TMD correlator

$$\bar{\Phi}_{\text{unsubtr.}}^{[\Gamma]}(b, P, S, \dots) \equiv \frac{1}{2} \langle P, S | \bar{q}(0) \Gamma \mathcal{U}[0, \dots, b] q(b) | P, S \rangle$$

$$\Phi^{[\Gamma]}(x, k_T, P, S, \dots) \equiv \int \frac{d^2 b_T}{(2\pi)^2} \int \frac{d(b \cdot P)}{(2\pi) P^+} \exp(ix(b \cdot P) - ib_T \cdot k_T) \left. \frac{\bar{\Phi}_{\text{unsubtr.}}^{[\Gamma]}(b, P, S, \dots)}{\bar{\mathcal{S}}(b^2, \dots)} \right|_{b^+=0}$$

- “Soft factor” $\bar{\mathcal{S}}$ required to subtract divergences of Wilson line \mathcal{U}
- $\bar{\mathcal{S}}$ is typically a combination of vacuum expectation values of Wilson line structures
- Here, will consider only ratios in which soft factors cancel

Gauge link structure motivated by SIDIS

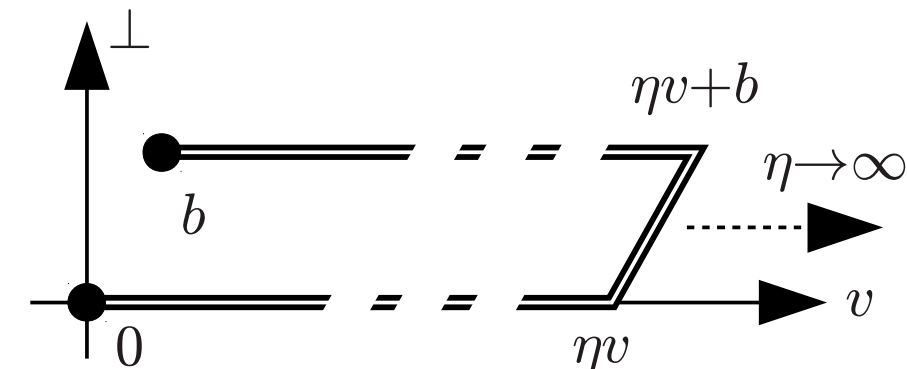


$$l + H(P) \longrightarrow l' + h(P_h) + X$$

Gauge link structure:

In matrix element $\tilde{\Phi}_{\text{unsubstr.}}^{[\Gamma]}(b, P, S, \dots) \equiv \frac{1}{2} \langle P, S | \bar{q}(0) \Gamma \mathcal{U}[0, \dots, b] q(b) | P, S \rangle$

Staple-shaped gauge link $\mathcal{U}[0, \eta v, \eta v + b, b]$



incorporates SIDIS final state effects

Gauge link structure motivated by SIDIS

Staple-shaped links incorporate SIDIS final state effects:

- Gauge link roughly follows direction of ejected quark, (close to) light cone
- Effective resummed description of gluon exchanges between ejected quark and remainder of nucleon in evolving final state
- Beyond tree level: Rapidity divergences suggest taking staple direction slightly off the light cone. Approach of Aybat, Collins, Qiu, Rogers makes v space-like. Parametrize in terms of Collins-Soper parameter

$$\hat{\zeta} \equiv \frac{P \cdot v}{|P||v|}$$

Light-like staple for $\hat{\zeta} \rightarrow \infty$. Perturbative evolution equations for large $\hat{\zeta}$.

Fundamental TMD correlator

$$\bar{\Phi}_{\text{unsubtr.}}^{[\Gamma]}(b, P, S, \dots) \equiv \frac{1}{2} \langle P, S | \bar{q}(0) \Gamma \mathcal{U}[0, \eta v, \eta v + b, b] q(b) | P, S \rangle$$

$$\Phi^{[\Gamma]}(x, k_T, P, S, \dots) \equiv \int \frac{d^2 b_T}{(2\pi)^2} \int \frac{d(b \cdot P)}{(2\pi) P^+} \exp(ix(b \cdot P) - ib_T \cdot k_T) \frac{\bar{\Phi}_{\text{unsubtr.}}^{[\Gamma]}(b, P, S, \dots)}{\bar{\mathcal{S}}(b^2, \dots)} \Big|_{b^+=0}$$

- “Soft factor” $\bar{\mathcal{S}}$ required to subtract divergences of Wilson line \mathcal{U}
- $\bar{\mathcal{S}}$ is typically a combination of vacuum expectation values of Wilson line structures
- Here, will consider only ratios in which soft factors cancel

Decomposition of Φ into TMDs

All leading twist structures:

$$\Phi^{[\gamma^+]} = f_1 - \left[\frac{\epsilon_{ij} k_i S_j}{m_H} f_{1T}^\perp \right]_{\text{odd}}$$

$$\Phi^{[\gamma^+ \gamma^5]} = \Lambda g_1 + \frac{k_T \cdot S_T}{m_H} g_{1T}$$

$$\Phi^{[i\sigma^{i+} \gamma^5]} = S_i h_1 + \frac{(2k_i k_j - k_T^2 \delta_{ij}) S_j}{2m_H^2} h_{1T}^\perp + \frac{\Lambda k_i}{m_H} h_{1L}^\perp + \left[\frac{\epsilon_{ij} k_j}{m_H} h_1^\perp \right]_{\text{odd}}$$

TMD Classification

All leading twist structures:

H ↓	$q \rightarrow$	U	L	T
U	f_1			h_1^\perp
L			g_1	h_{1L}^\perp
T		f_{1T}^\perp	g_{1T}	h_1 h_{1T}^\perp

↑
Sivers (T-odd)

← Boer-Mulders
(T-odd)

Decomposition of $\widetilde{\Phi}$ into amplitudes

$$\widetilde{\Phi}_{\text{unsubtr.}}^{[\Gamma]}(b, P, S, \hat{\zeta}, \mu) \equiv \frac{1}{2} \langle P, S | \bar{q}(0) \Gamma \mathcal{U}[0, \eta v, \eta v + b, b] q(b) | P, S \rangle$$

Decompose in terms of invariant amplitudes; at leading twist,

$$\frac{1}{2P^+} \widetilde{\Phi}_{\text{unsubtr.}}^{[\gamma^+]} = \bar{A}_{2B} + im_H \epsilon_{ij} b_i S_j \bar{A}_{12B}$$

$$\frac{1}{2P^+} \widetilde{\Phi}_{\text{unsubtr.}}^{[\gamma^+ \gamma^5]} = -\Lambda \bar{A}_{6B} + i[(b \cdot P)\Lambda - m_H(b_T \cdot S_T)] \bar{A}_{7B}$$

$$\begin{aligned} \frac{1}{2P^+} \widetilde{\Phi}_{\text{unsubtr.}}^{[i\sigma^{i+} \gamma^5]} &= im_H \epsilon_{ij} b_j \bar{A}_{4B} - S_i \bar{A}_{9B} \\ &\quad - im_H \Lambda b_i \bar{A}_{10B} + m_H[(b \cdot P)\Lambda - m_H(b_T \cdot S_T)] b_i \bar{A}_{11B} \end{aligned}$$

(Decompositions analogous to work by Metz et al. in momentum space)

Fourier-transformed TMDs

$$\tilde{f}(x, b_T^2, \dots) \equiv \int d^2 k_T \exp(ib_T \cdot k_T) f(x, k_T^2, \dots)$$

$$\tilde{f}^{(n)}(x, b_T^2, \dots) \equiv n! \left(-\frac{2}{m_H^2} \partial_{b_T^2} \right)^n \tilde{f}(x, b_T^2, \dots)$$

In limit $|b_T| \rightarrow 0$, recover k_T -moments:

$$\tilde{f}^{(n)}(x, 0, \dots) \equiv \int d^2 k_T \left(\frac{k_T^2}{2m_H^2} \right)^n f(x, k_T^2, \dots) \equiv f^{(n)}(x)$$

ill-defined for large k_T , so will not attempt to extrapolate to $b_T = 0$, but give results at finite $|b_T|$.

In this study, only consider first x -moments (accessible at $b \cdot P = 0$), rather than scanning range of $b \cdot P$:

$$f^{[1]}(k_T^2, \dots) \equiv \int_{-1}^1 dx f(x, k_T^2, \dots)$$

→ Bessel-weighted asymmetries (Boer, Gamberg, Musch, Prokudin, JHEP 1110 (2011) 021)

Relation between Fourier-transformed TMDs and invariant amplitudes \bar{A}_i

Invariant amplitudes directly give selected x -integrated TMDs in Fourier (b_T) space (showing just the ones relevant for Sivers, Boer-Mulders shifts), up to soft factors:

$$\tilde{f}_1^{[1](0)}(b_T^2, \hat{\zeta}, \dots, \eta v \cdot P) = 2\bar{A}_{2B}(-b_T^2, 0, \hat{\zeta}, \eta v \cdot P)/\bar{S}(b^2, \dots)$$

$$\tilde{f}_{1T}^{\perp1}(b_T^2, \hat{\zeta}, \dots, \eta v \cdot P) = -2\bar{A}_{12B}(-b_T^2, 0, \hat{\zeta}, \eta v \cdot P)/\bar{S}(b^2, \dots)$$

$$\tilde{h}_1^{\perp1}(b_T^2, \hat{\zeta}, \dots, \eta v \cdot P) = 2\bar{A}_{4B}(-b_T^2, 0, \hat{\zeta}, \eta v \cdot P)/\bar{S}(b^2, \dots)$$

Generalized shifts

Form ratios in which soft factors, (Γ -independent) multiplicative renormalization factors cancel

Boer-Mulders shift:

$$\langle k_y \rangle_{UT} \equiv m_H \frac{\tilde{h}_1^{\perp1}}{\tilde{f}_1^{[1](0)}} = \left. \frac{\int dx \int d^2 k_T k_y \Phi[\gamma^+ + s^j i\sigma^j + \gamma^5](x, k_T, P, \dots)}{\int dx \int d^2 k_T \Phi[\gamma^+ + s^j i\sigma^j + \gamma^5](x, k_T, P, \dots)} \right|_{s_T=(1,0)}$$

Average transverse momentum of quarks polarized in the orthogonal transverse (“ T ”) direction in an unpolarized (“ U ”) hadron; normalized to the number of valence quarks. “Dipole moment” in $b_T^2 = 0$ limit, “shift”.

Issue: k_T -moments in this ratio singular; generalize to ratio of Fourier-transformed TMDs at *nonzero* b_T^2 ,

$$\langle k_y \rangle_{UT}(b_T^2, \dots) \equiv m_H \frac{\tilde{h}_1^{\perp1}(b_T^2, \dots)}{\tilde{f}_1^{[1](0)}(b_T^2, \dots)}$$

(remember singular $b_T \rightarrow 0$ limit corresponds to taking k_T -moment). “Generalized shift”.

Generalized shifts from amplitudes

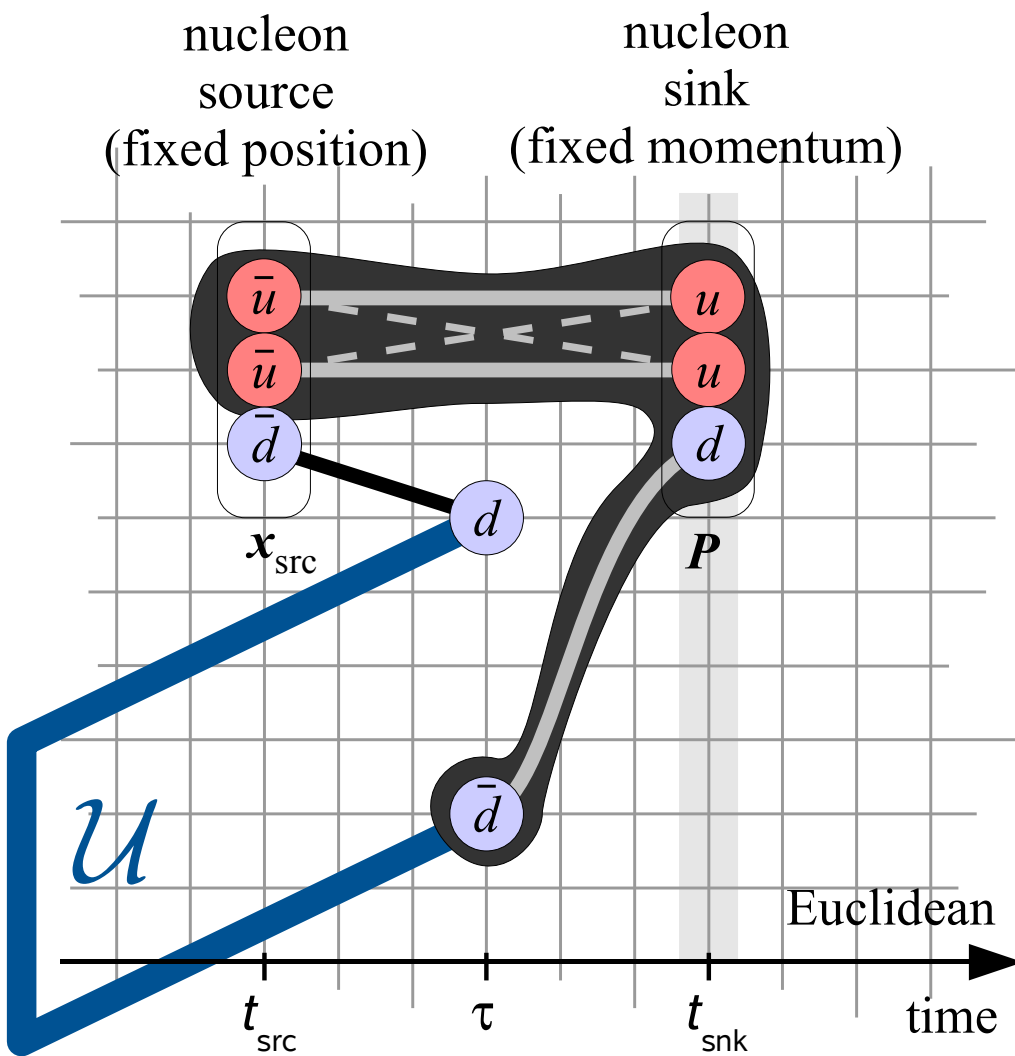
Now, can also express this in terms of invariant amplitudes:

$$\langle k_y \rangle_{UT}(b_T^2, \dots) \equiv m_H \frac{\tilde{h}_1^{\perp1}(b_T^2, \dots)}{\tilde{f}_1^{[1](0)}(b_T^2, \dots)} = m_H \frac{\bar{A}_{4B}(-b_T^2, 0, \hat{\zeta}, \eta v \cdot P)}{\bar{A}_{2B}(-b_T^2, 0, \hat{\zeta}, \eta v \cdot P)}$$

Analogously, Sivers shift (in a polarized hadron):

$$\langle k_y \rangle_{TU}(b_T^2, \dots) = -m_H \frac{\bar{A}_{12B}(-b_T^2, 0, \hat{\zeta}, \eta v \cdot P)}{\bar{A}_{2B}(-b_T^2, 0, \hat{\zeta}, \eta v \cdot P)}$$

Lattice setup



- Evaluate directly $\bar{\Phi}_{\text{unsubtr.}}^{[\Gamma]}(b, P, S, \hat{\zeta}, \mu)$
 $\equiv \frac{1}{2} \langle P, S | \bar{q}(0) \Gamma \mathcal{U}[0, \eta v, \eta v + b, b] q(b) | P, S \rangle$
- Euclidean time: Place entire operator at one time slice, i.e., $b, \eta v$ purely spatial
- Since generic b, v space-like, no obstacle to boosting system to such a frame!
- Parametrization of correlator in terms of \bar{A}_i invariants permits direct translation of results back to original frame; form desired \bar{A}_i ratios.
- Use variety of $P, b, \eta v$; here $b \perp P, b \perp v$ (lowest x -moment, kinematical choices/constraints)
- Extrapolate $\eta \rightarrow \infty, \hat{\zeta} \rightarrow \infty$ numerically.

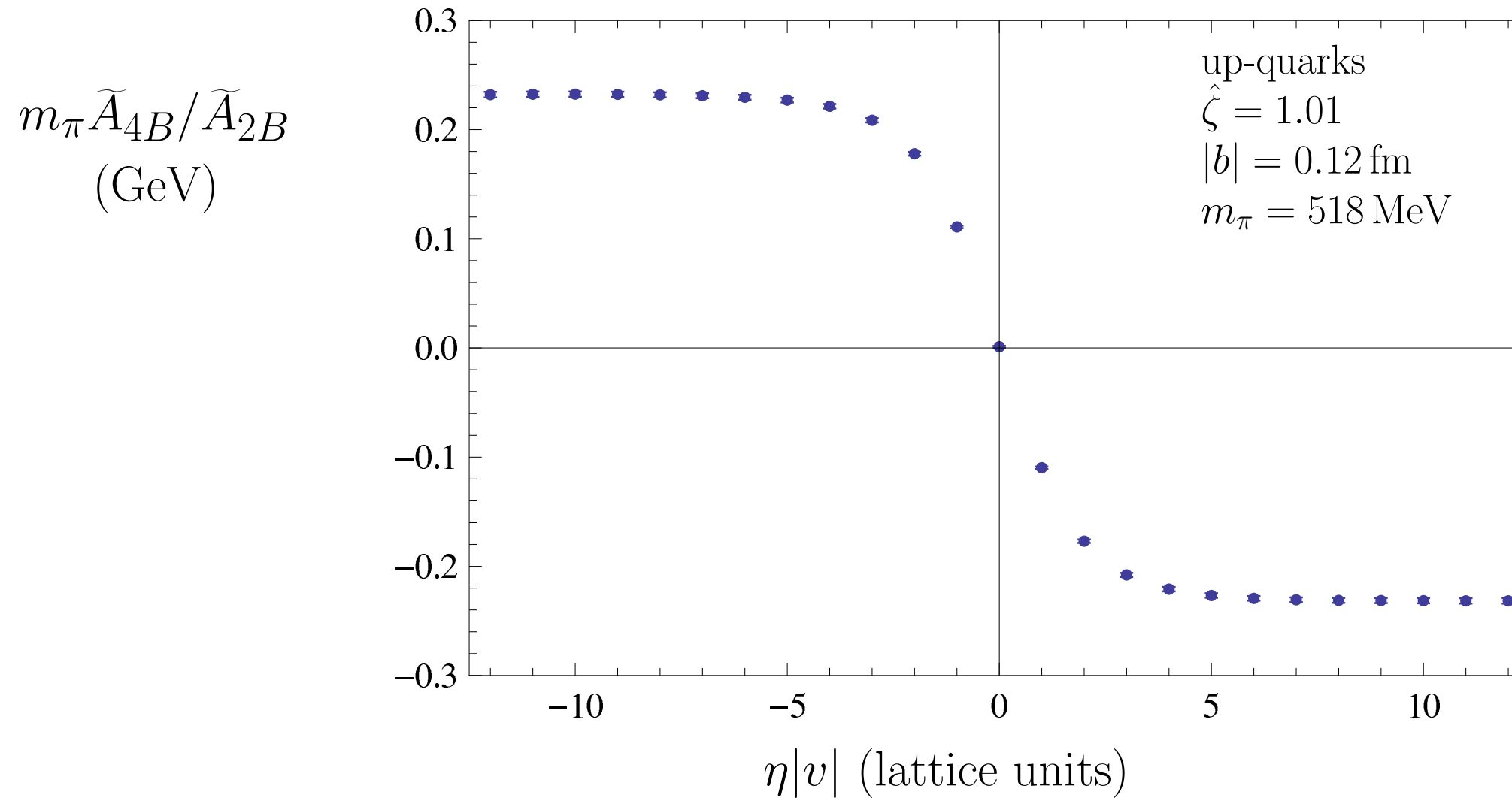
Challenges

- The limit $\hat{\zeta} \rightarrow \infty$: Approaching the light cone
- Discretization effects, soft factor cancellation on the lattice in TMD ratios
- Progress toward the physical pion mass

Approaching the light cone (with a pion)

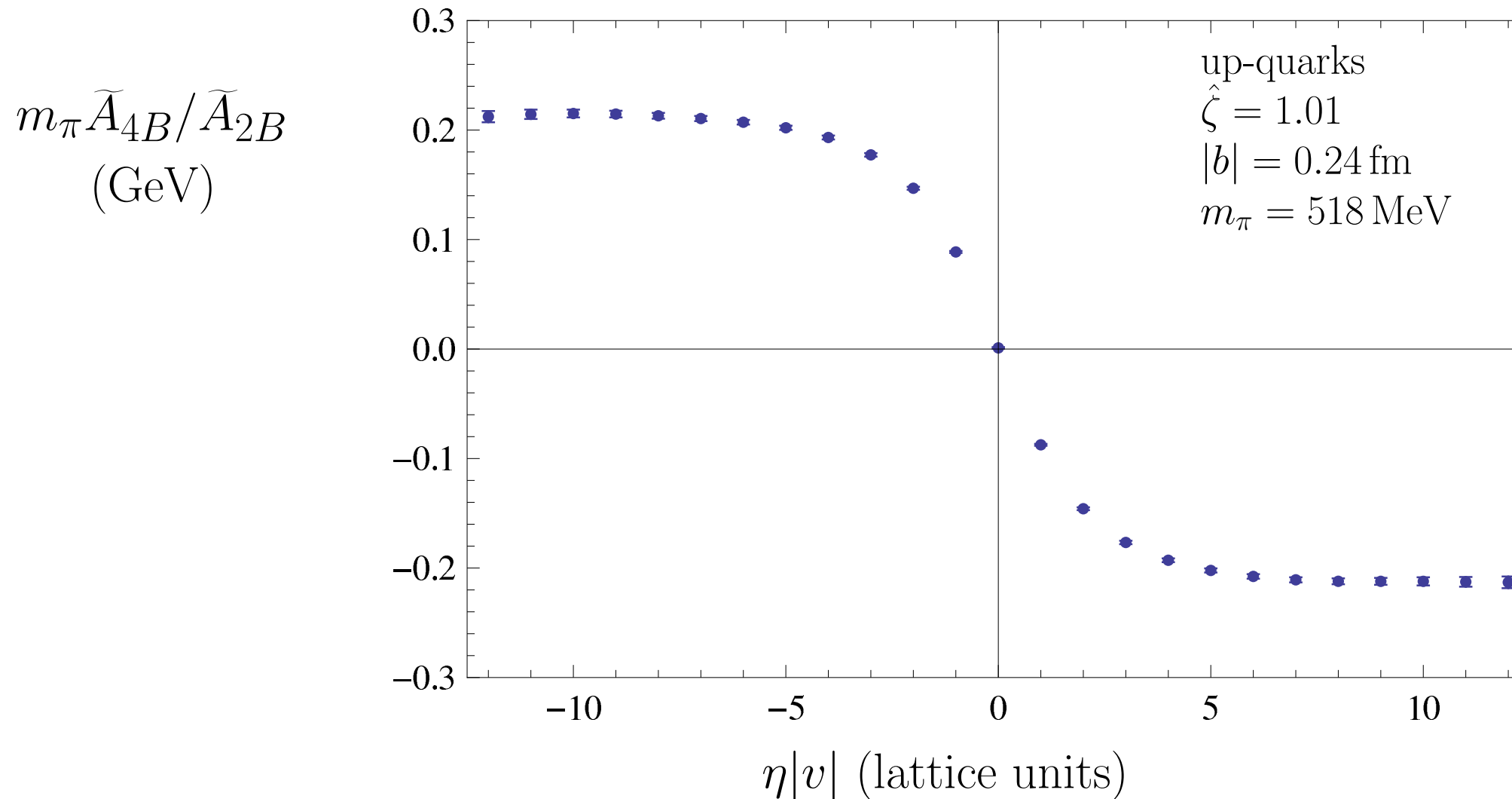
Results: Boer-Mulders shift (pion)

Dependence on staple extent; sequence of panels at different $|b_T|$



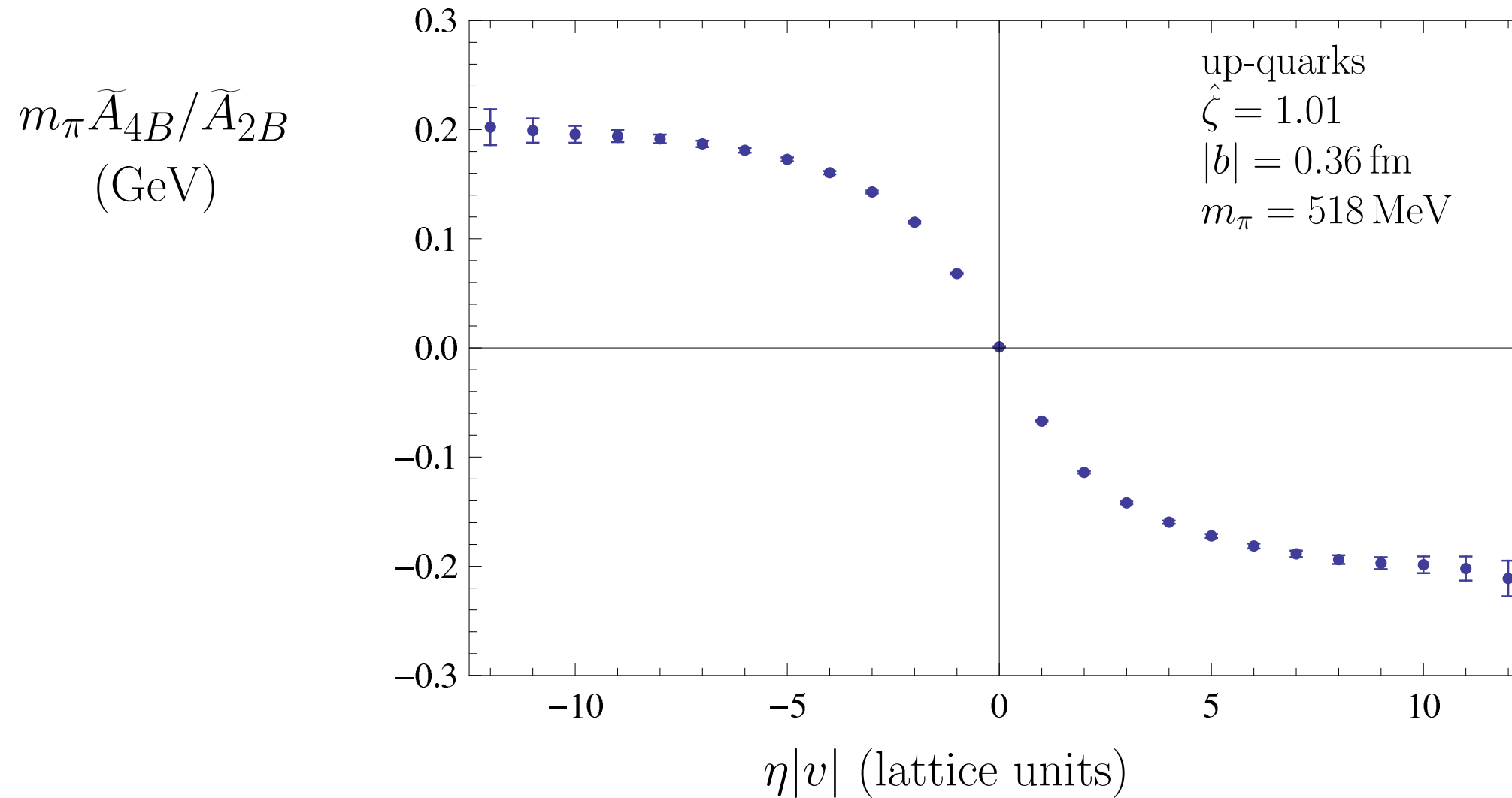
Results: Boer-Mulders shift (pion)

Dependence on staple extent; sequence of panels at different $|b_T|$



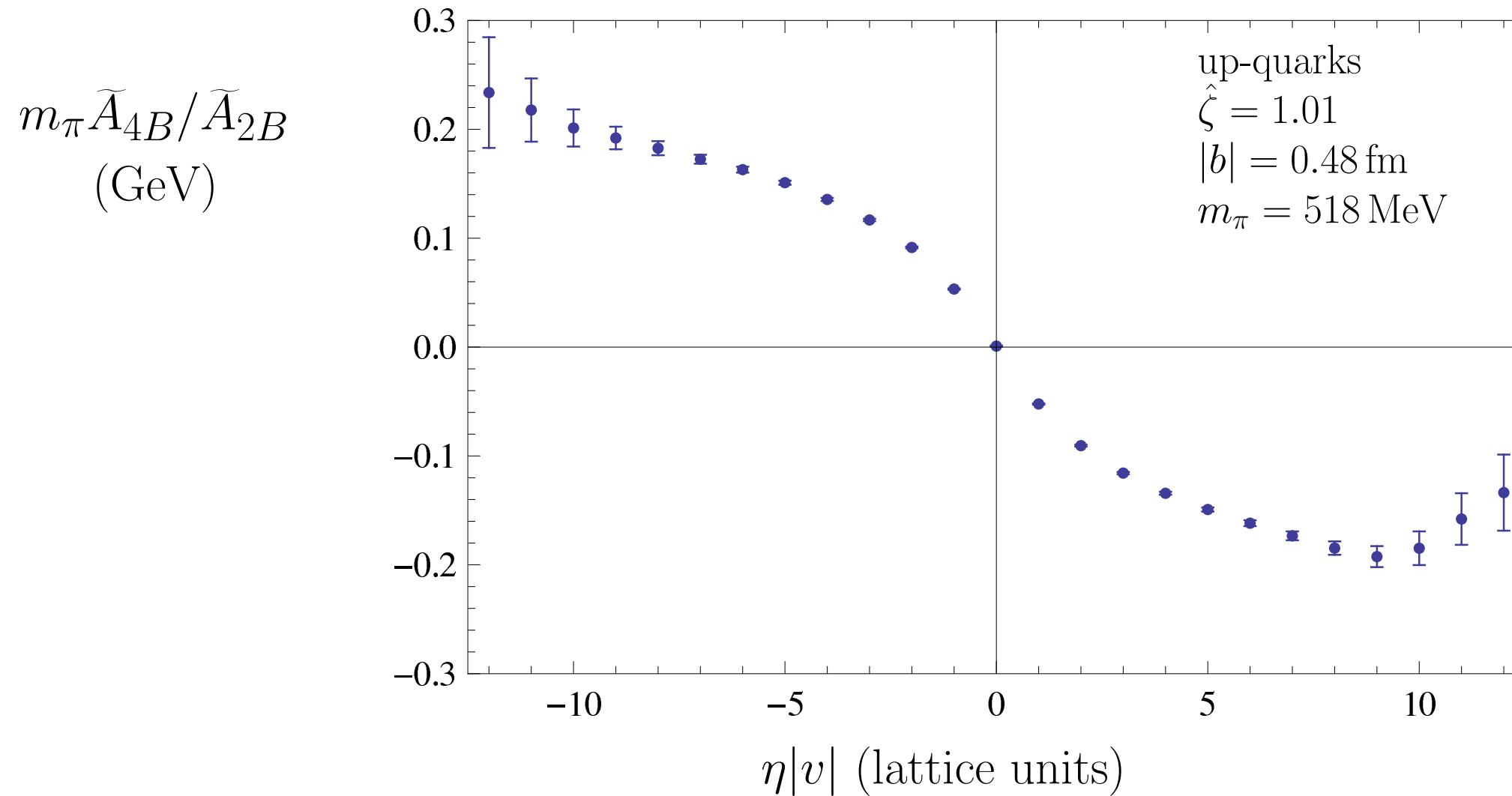
Results: Boer-Mulders shift (pion)

Dependence on staple extent; sequence of panels at different $|b_T|$



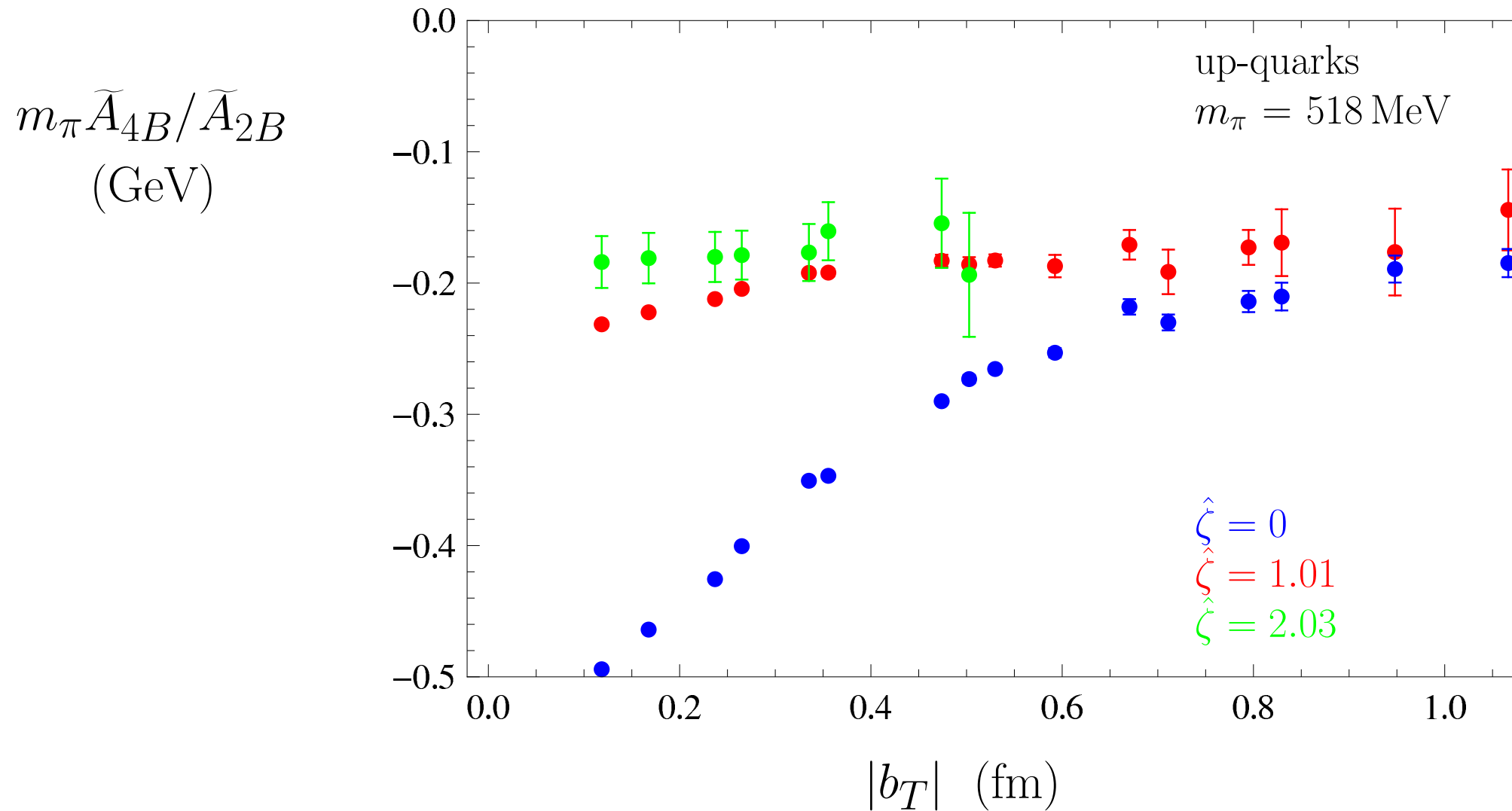
Results: Boer-Mulders shift (pion)

Dependence on staple extent; sequence of panels at different $|b_T|$



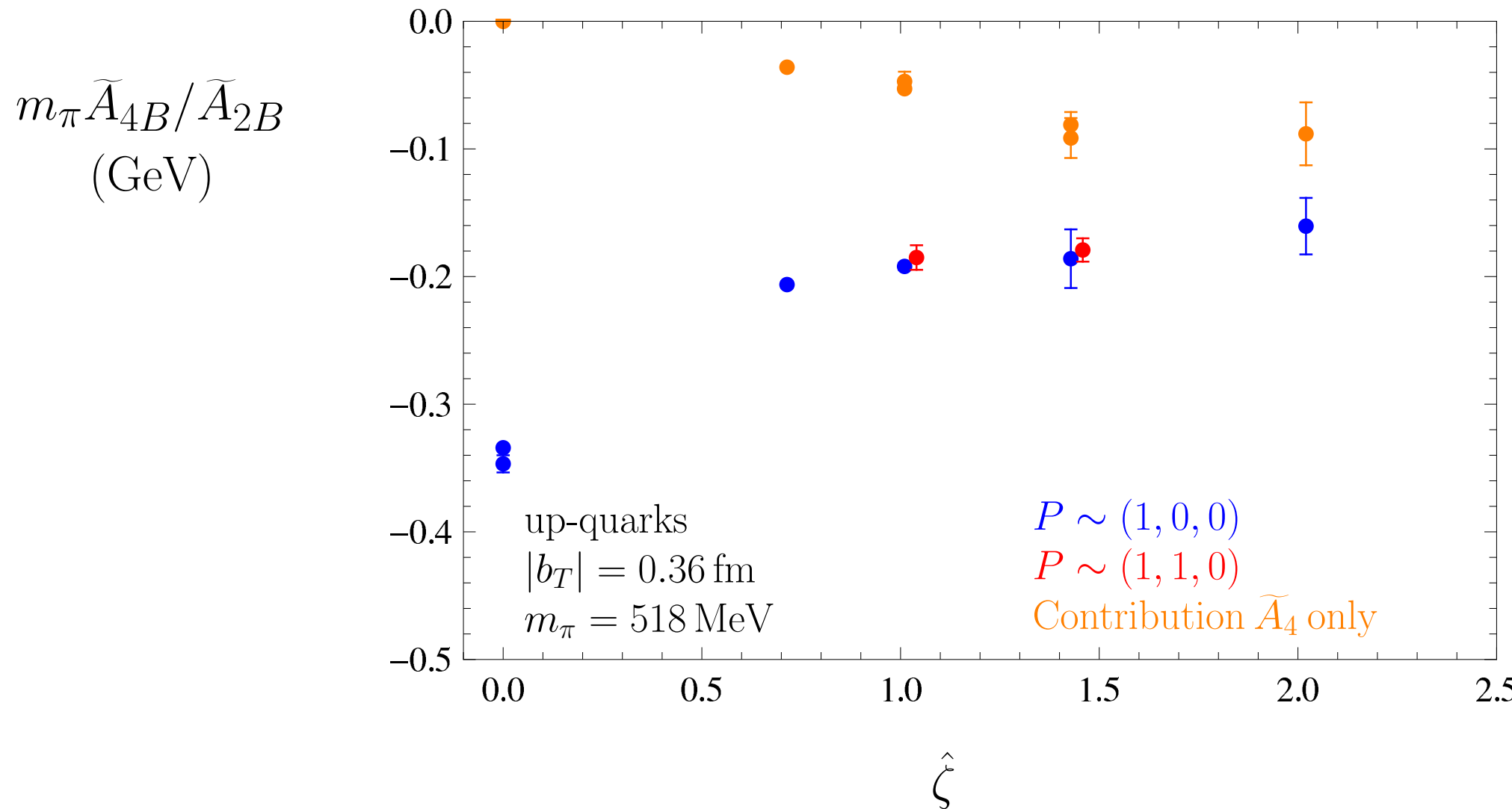
Results: Boer-Mulders shift (pion)

Dependence of SIDIS limit on $|b_T|$



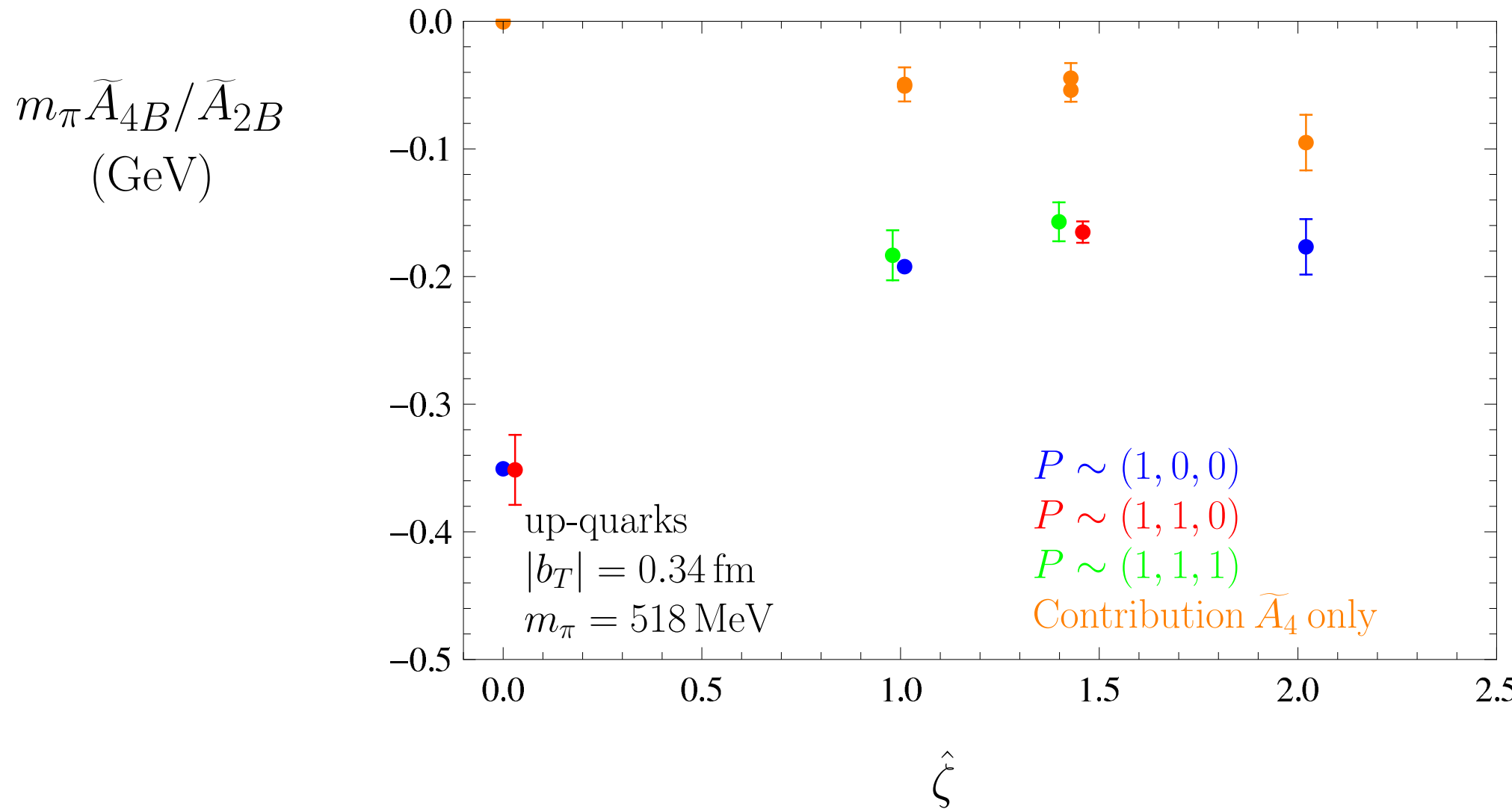
Results: Boer-Mulders shift (pion)

Dependence of SIDIS limit on $\hat{\zeta}$



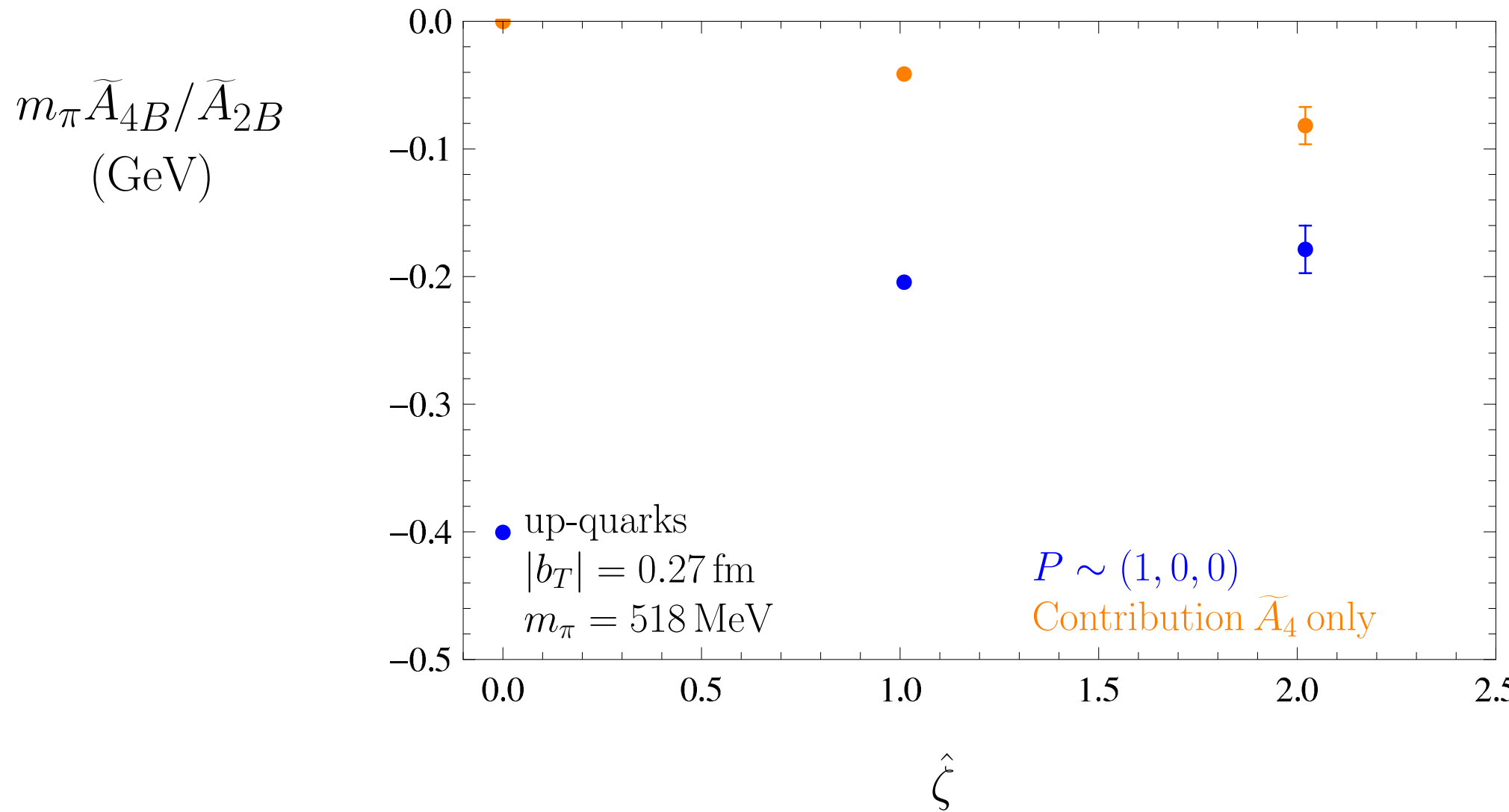
Results: Boer-Mulders shift (pion)

Dependence of SIDIS limit on $\hat{\zeta}$



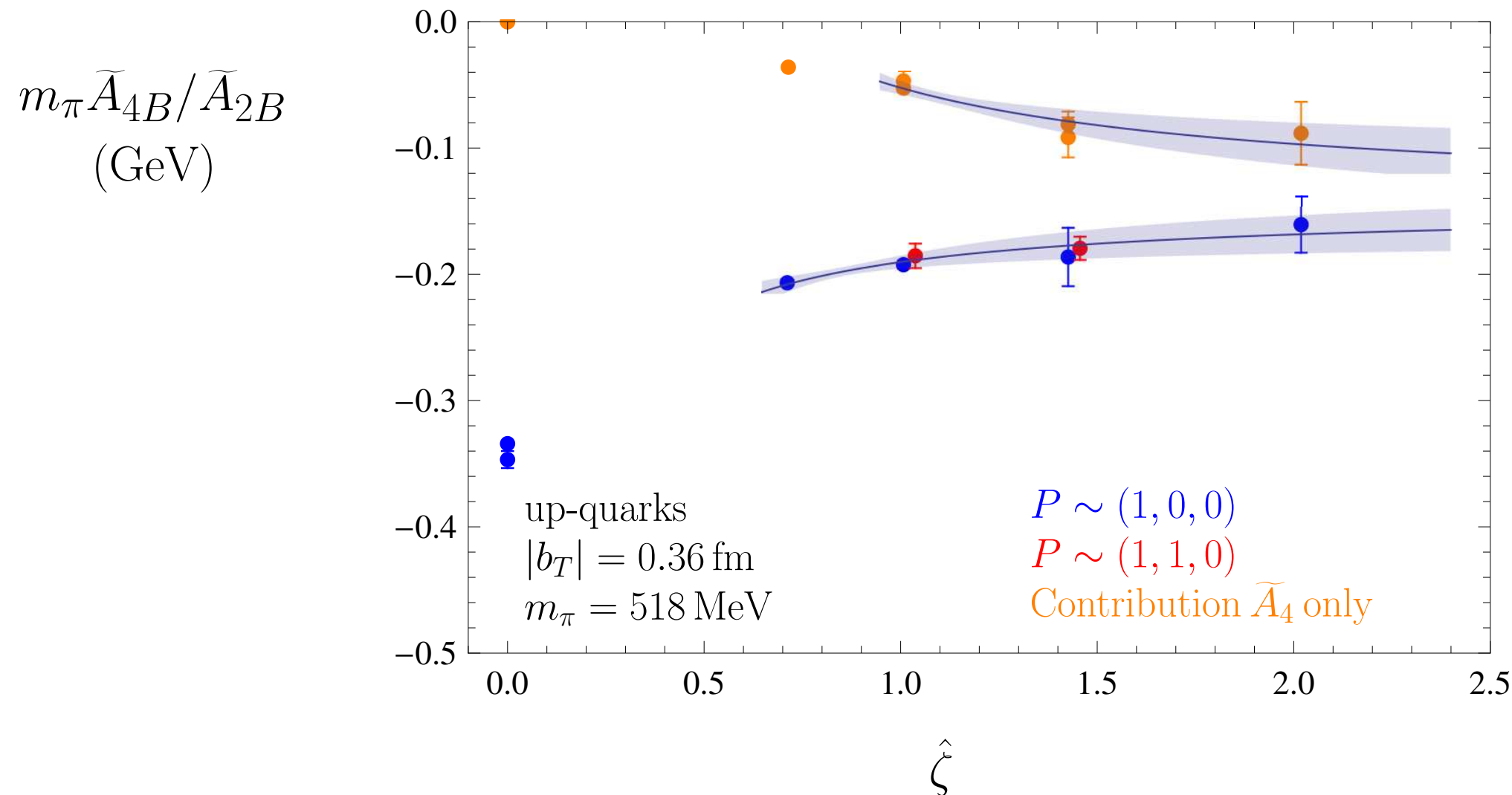
Results: Boer-Mulders shift (pion)

Dependence of SIDIS limit on $\hat{\zeta}$



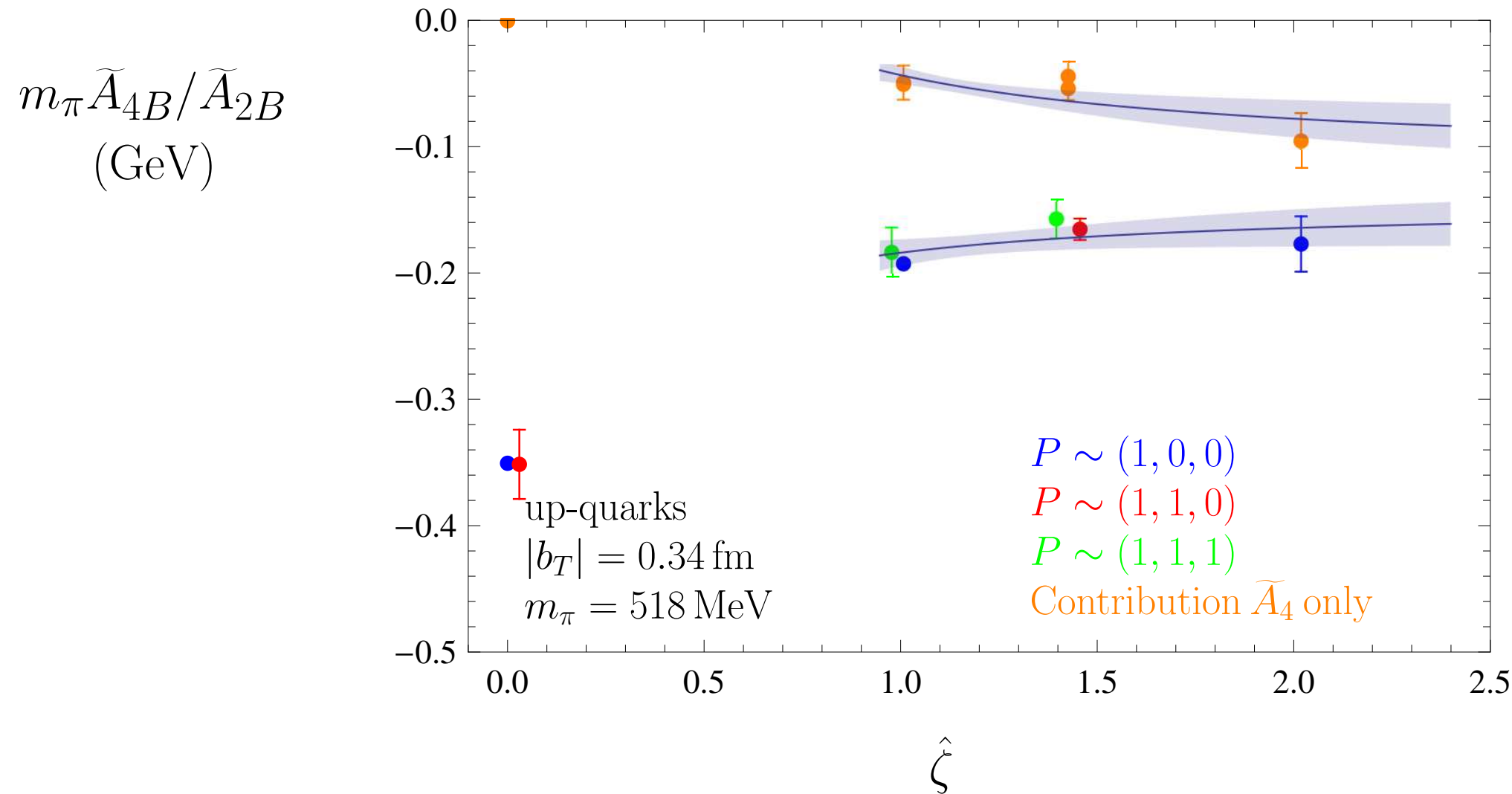
Results: Boer-Mulders shift (pion)

Dependence of SIDIS limit on $\hat{\zeta}$; fit function $a + b/\hat{\zeta}$



Results: Boer-Mulders shift (pion)

Dependence of SIDIS limit on $\hat{\zeta}$; fit function $a + b/\hat{\zeta}$



Results: Boer-Mulders shift (pion)

Extrapolation of SIDIS limit to $\hat{\zeta} \rightarrow \infty$

	Fit function	Full BM ratio (GeV)	Contribution \hat{A}_4 only (GeV)	Combined fit (GeV)	RMS deviation of combined fit (GeV)
$ b_T = 0.36 \text{ fm}$	$a + b/\hat{\zeta}$	-0.146(26)	-0.141(36)	-0.145(25)	0.00755
$ b_T = 0.36 \text{ fm}$	$a + b/\hat{\zeta}^2$	-0.166(16)	-0.110(22)	-0.148(15)	0.01695
$ b_T = 0.34 \text{ fm}$	$a + b/\hat{\zeta}$	-0.145(33)	-0.112(33)	-0.128(29)	0.01466
$ b_T = 0.34 \text{ fm}$	$a + b/\hat{\zeta}^2$	-0.157(19)	-0.084(19)	-0.121(16)	0.02315

up-quarks

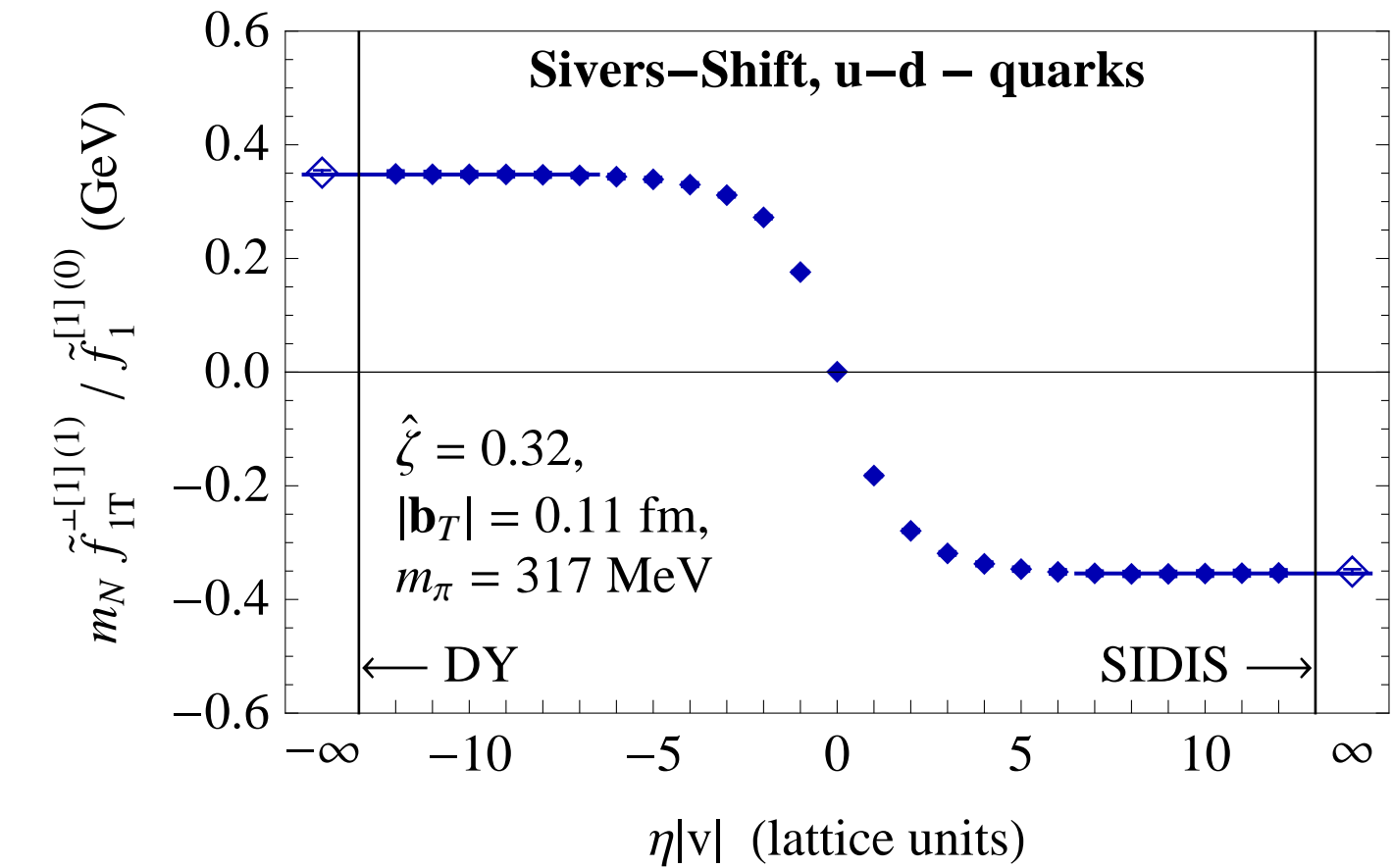
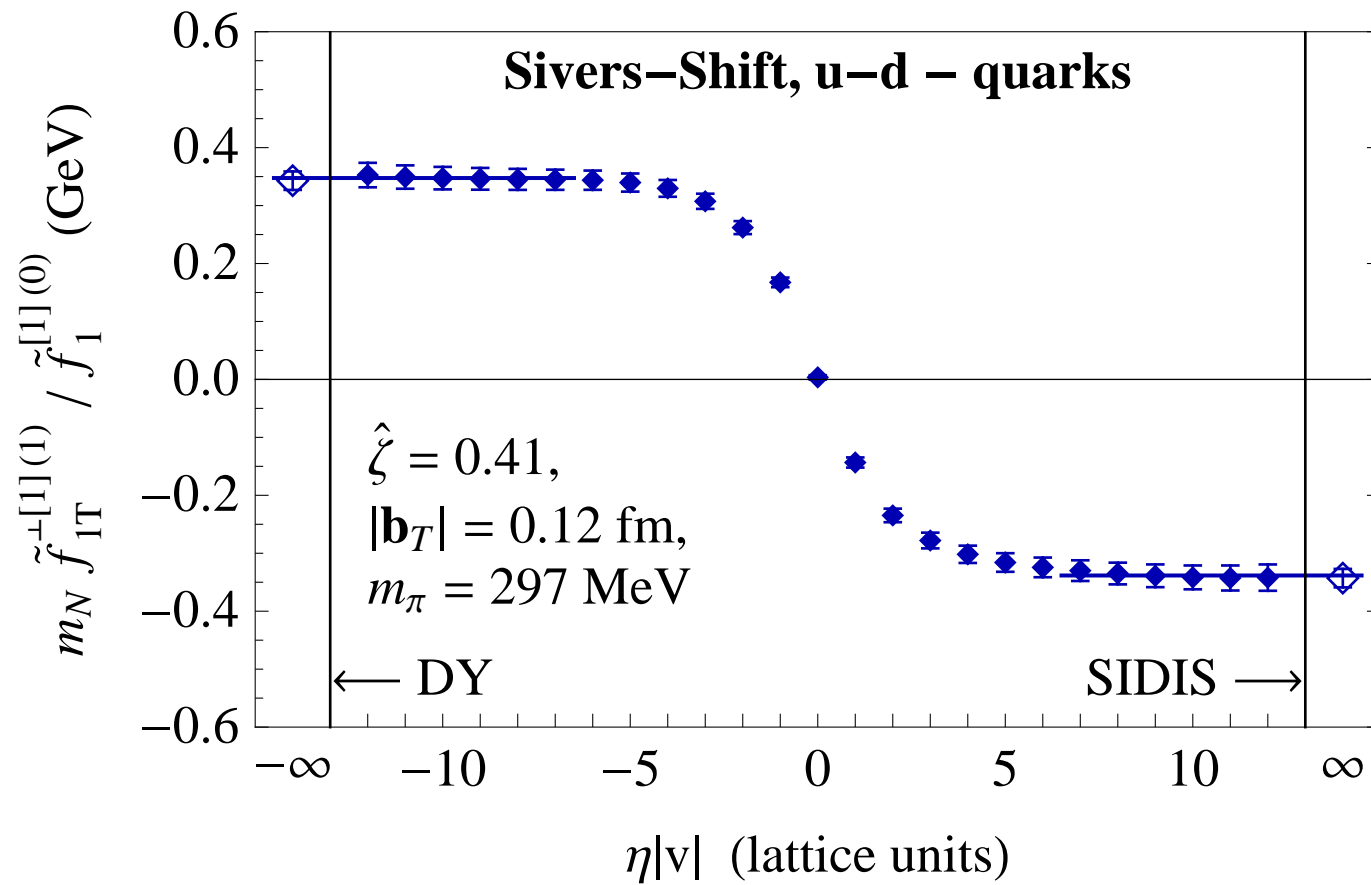
$m_\pi = 518 \text{ MeV}$

Discretization effects:

Comparison of RBC/UKQCD DWF ensemble ($m_\pi = 297 \text{ MeV}$, $a = 0.084 \text{ fm}$)
with USQCD clover ensemble ($m_\pi = 317 \text{ MeV}$, $a = 0.114 \text{ fm}$)

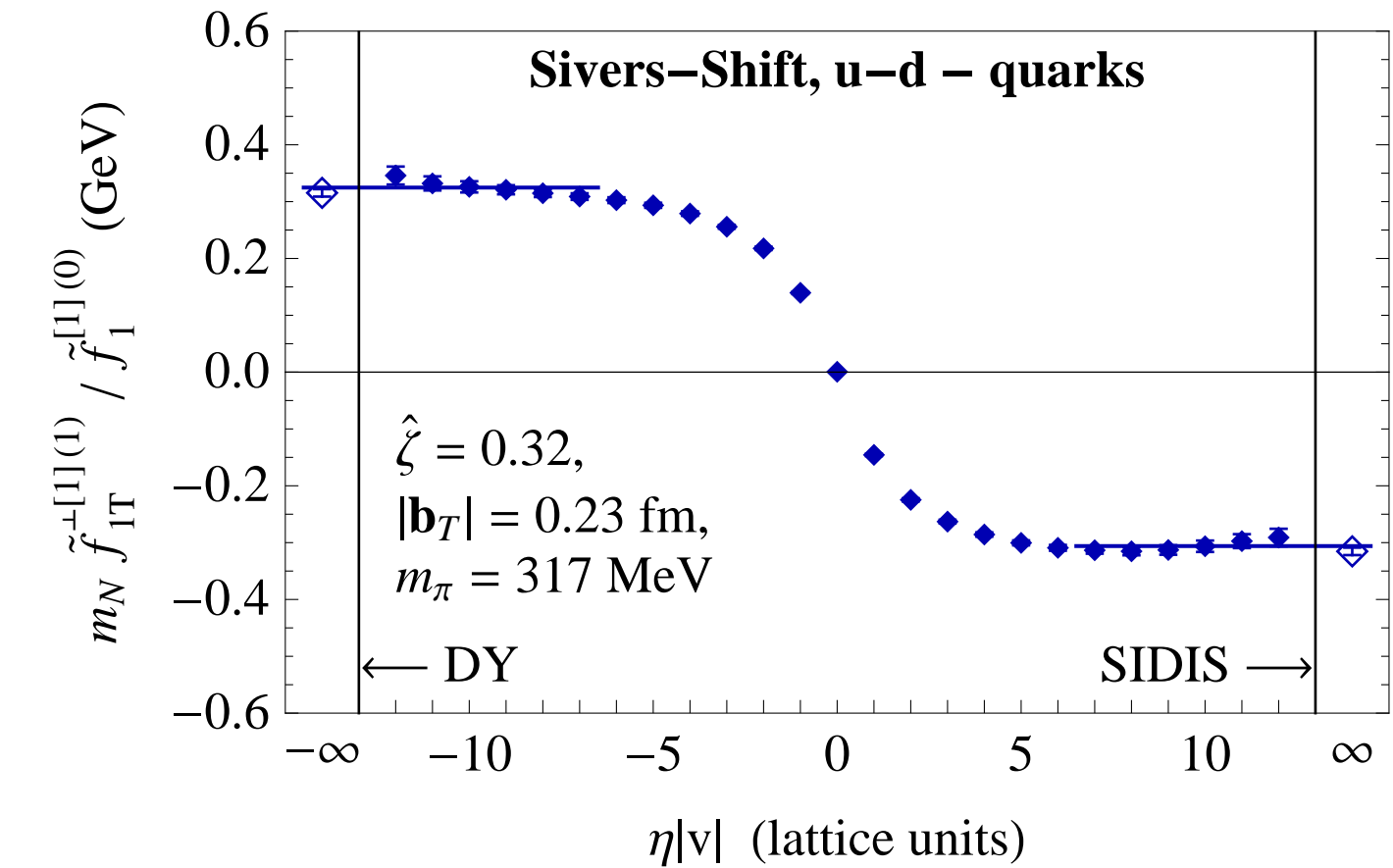
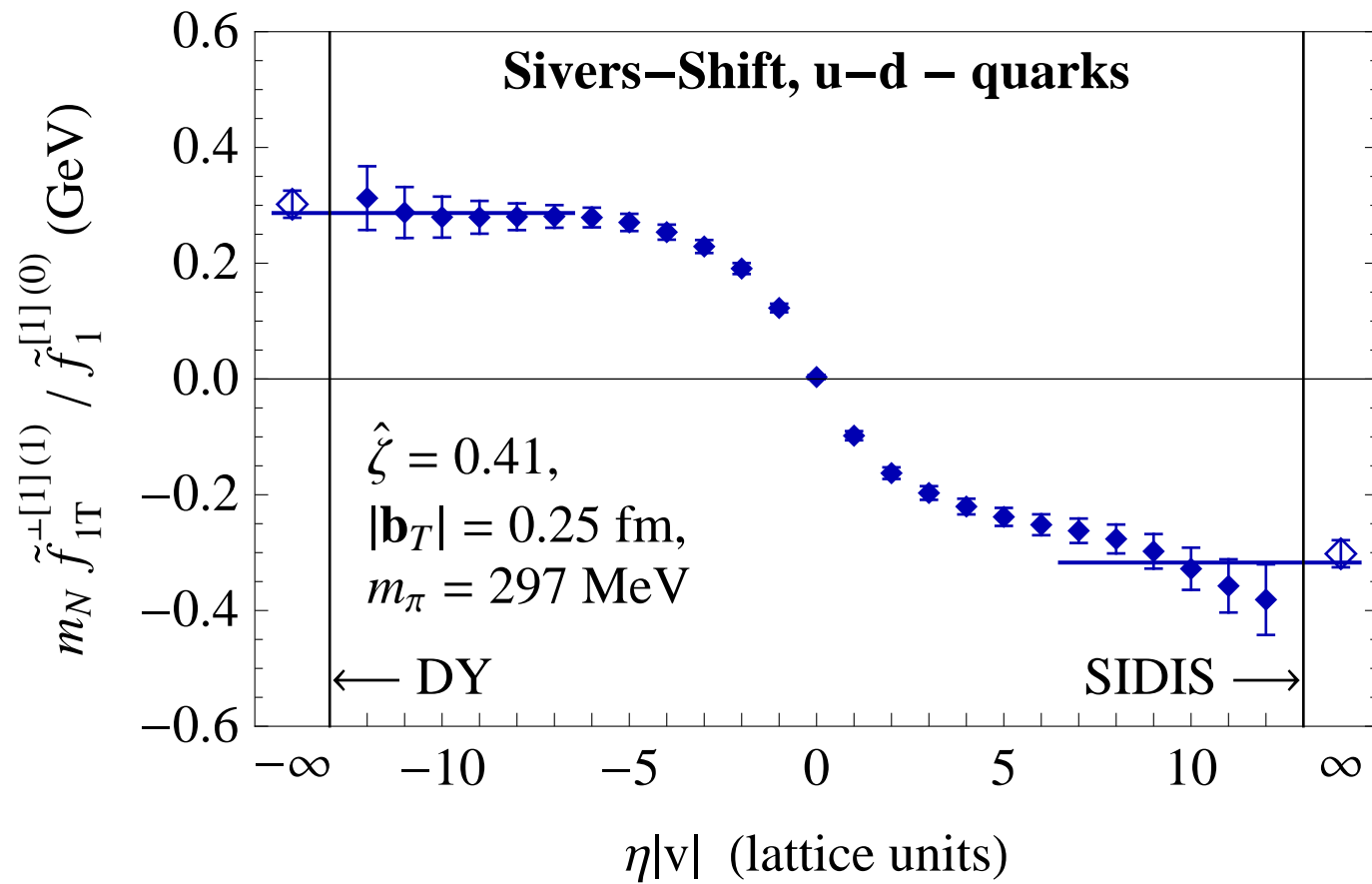
Results: Sivers shift

Dependence on staple extent; sequence of panels at different $|b_T|$



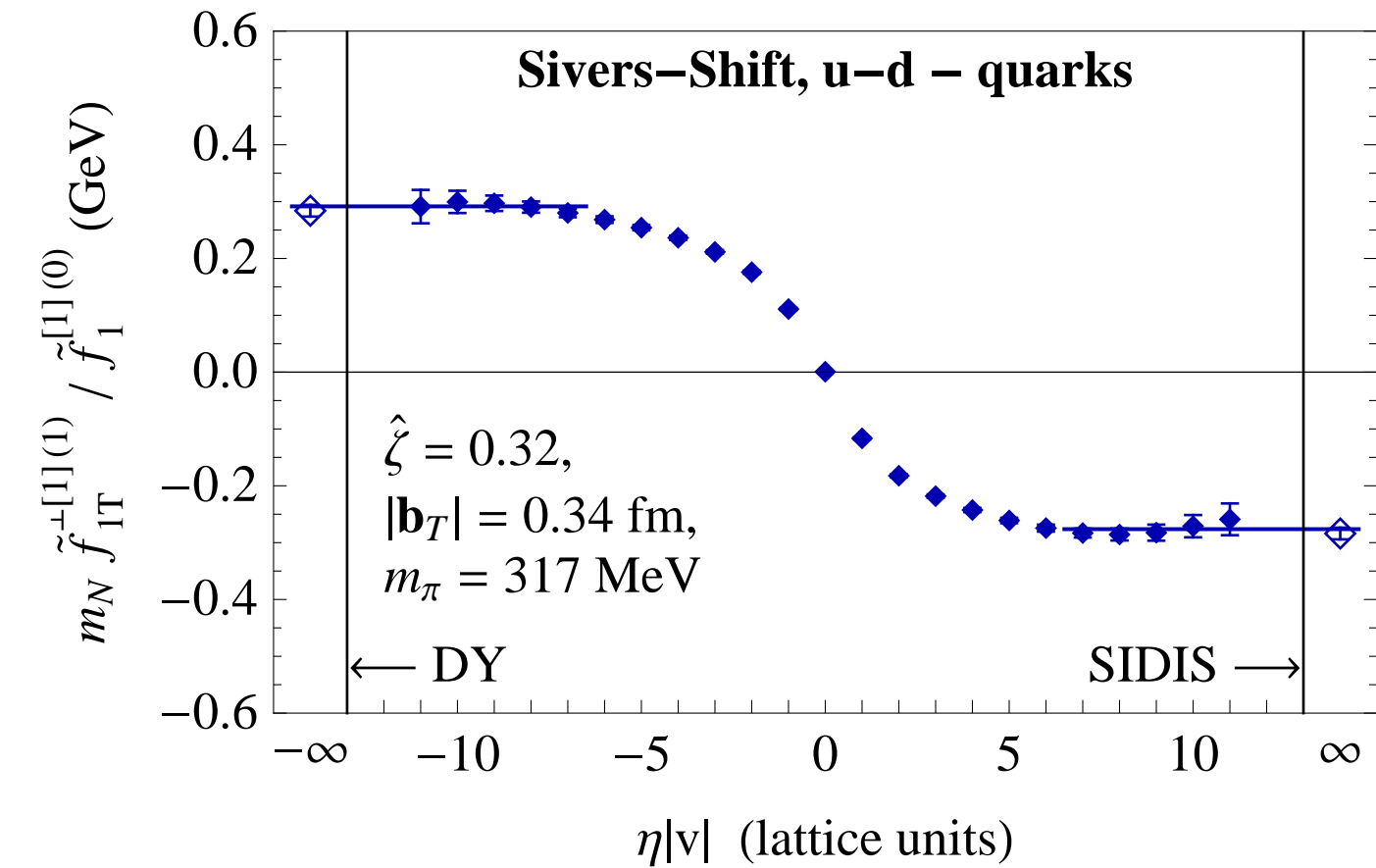
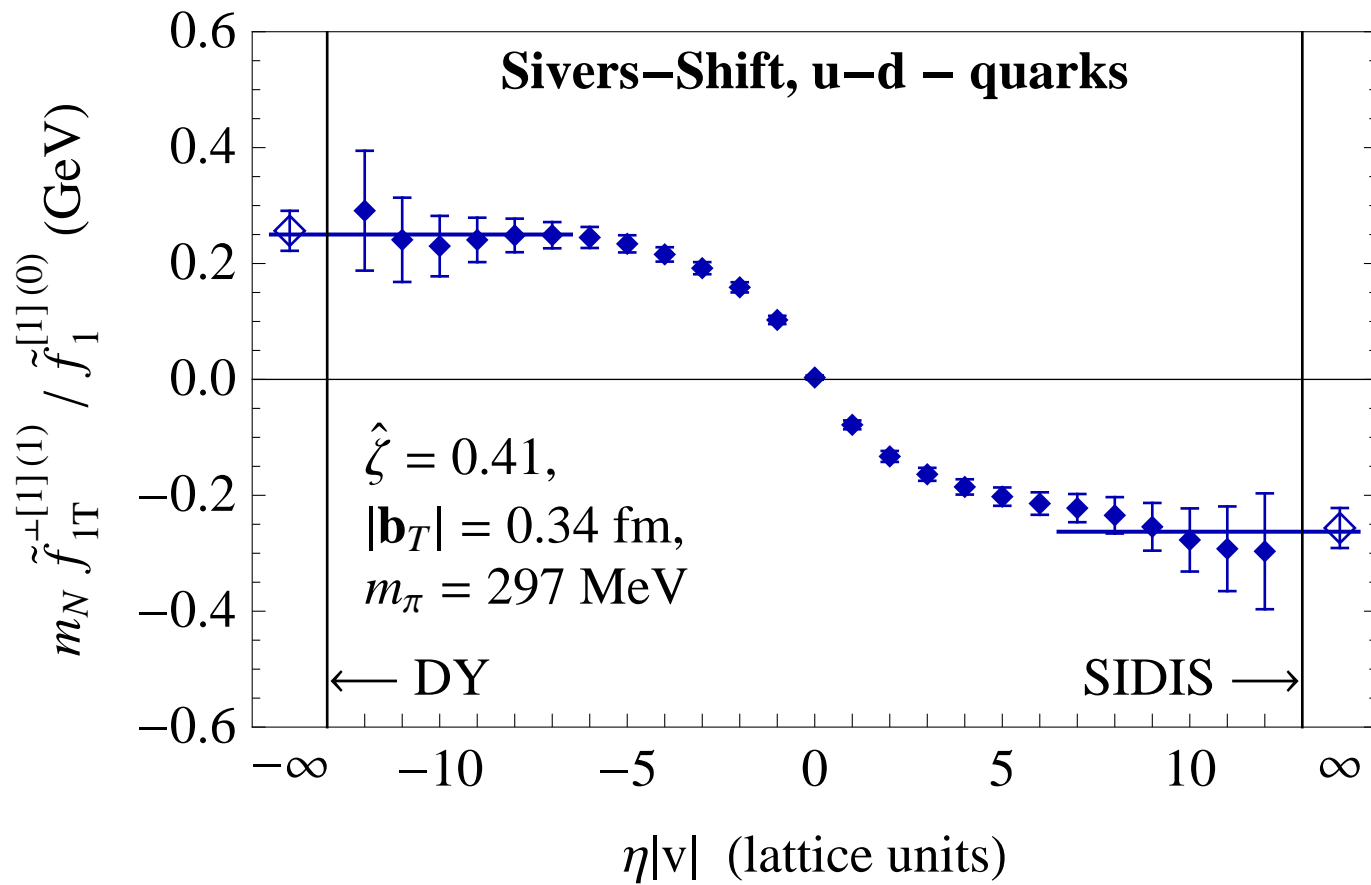
Results: Sivers shift

Dependence on staple extent; sequence of panels at different $|b_T|$



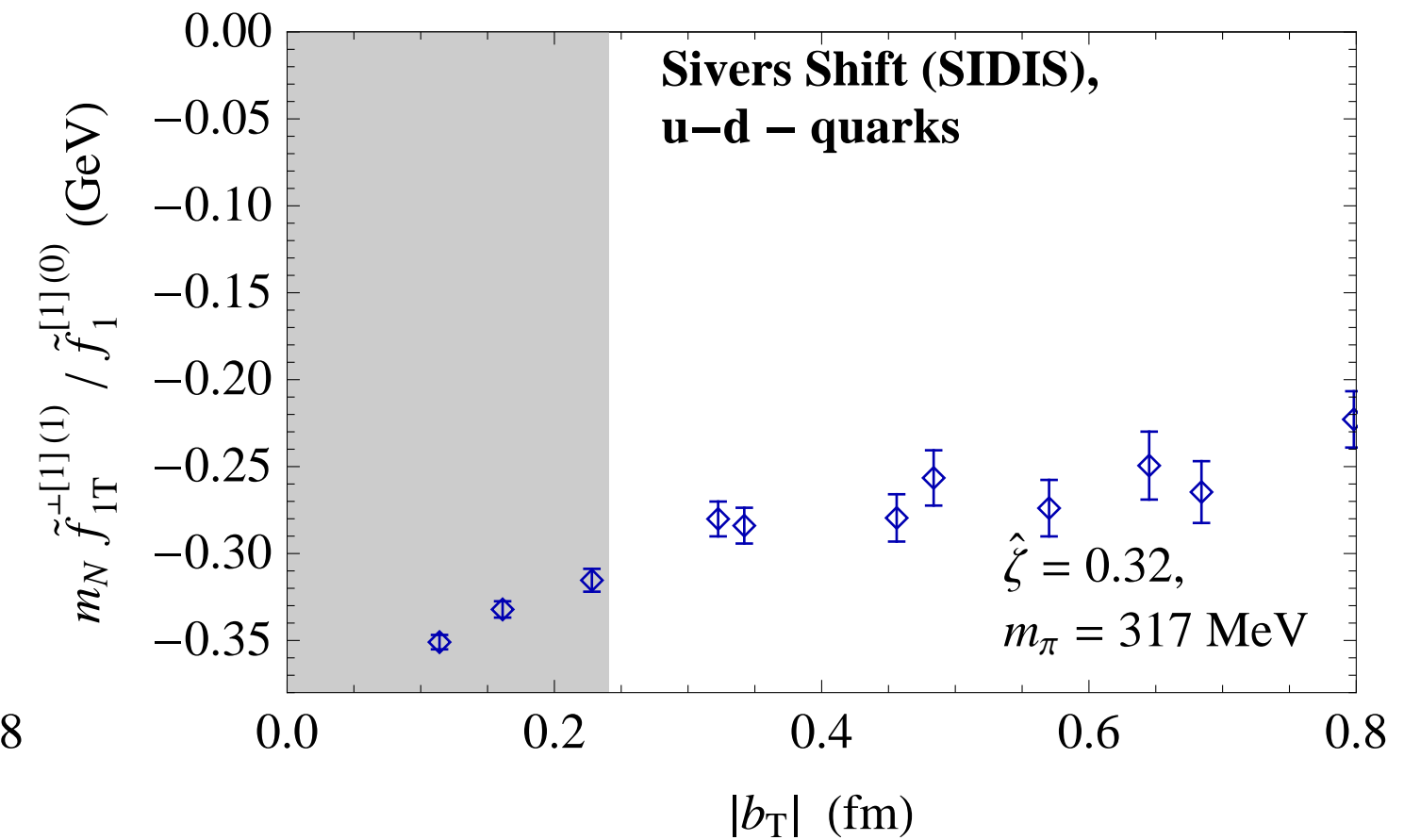
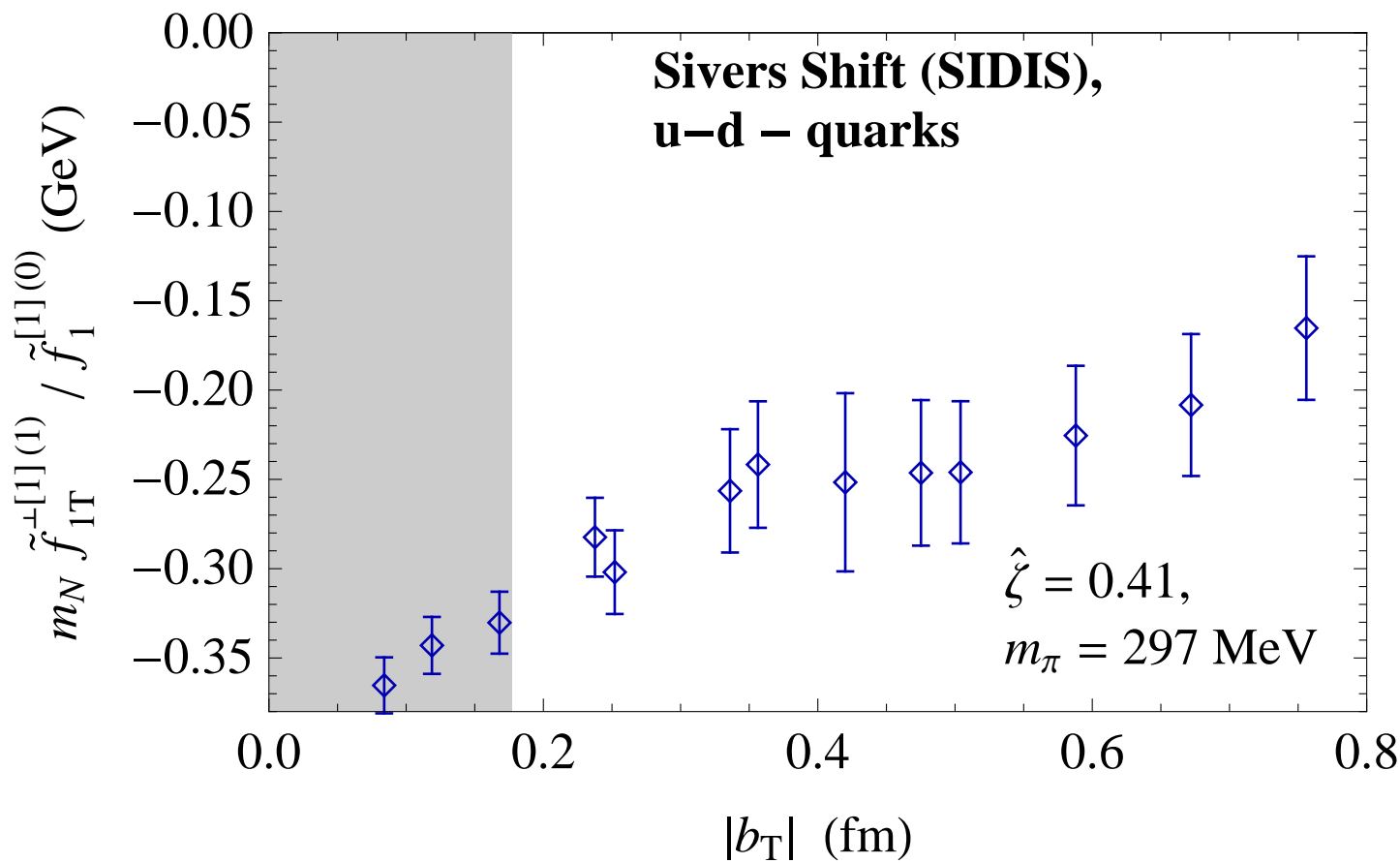
Results: Sivers shift

Dependence on staple extent; sequence of panels at different $|b_T|$



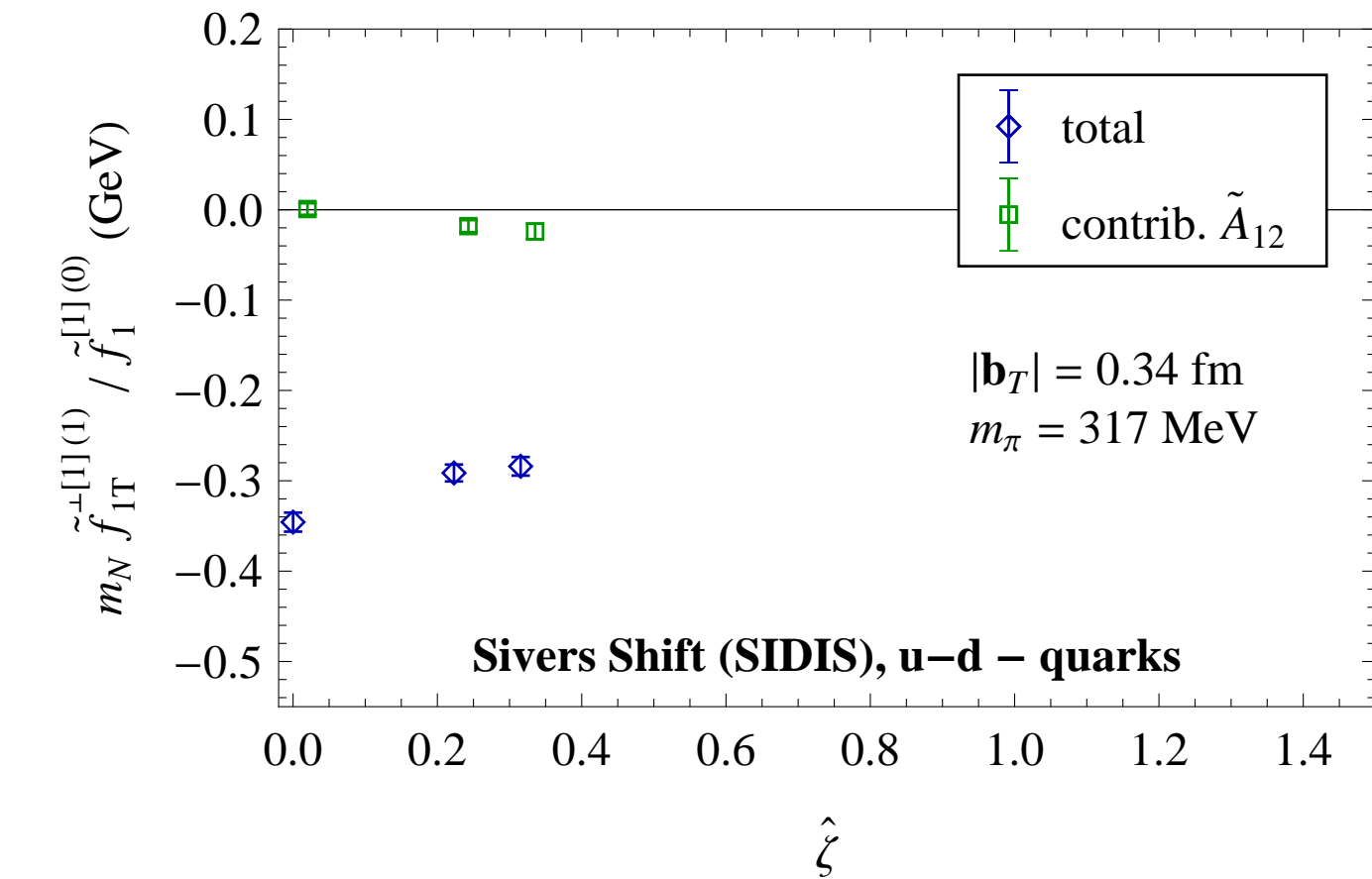
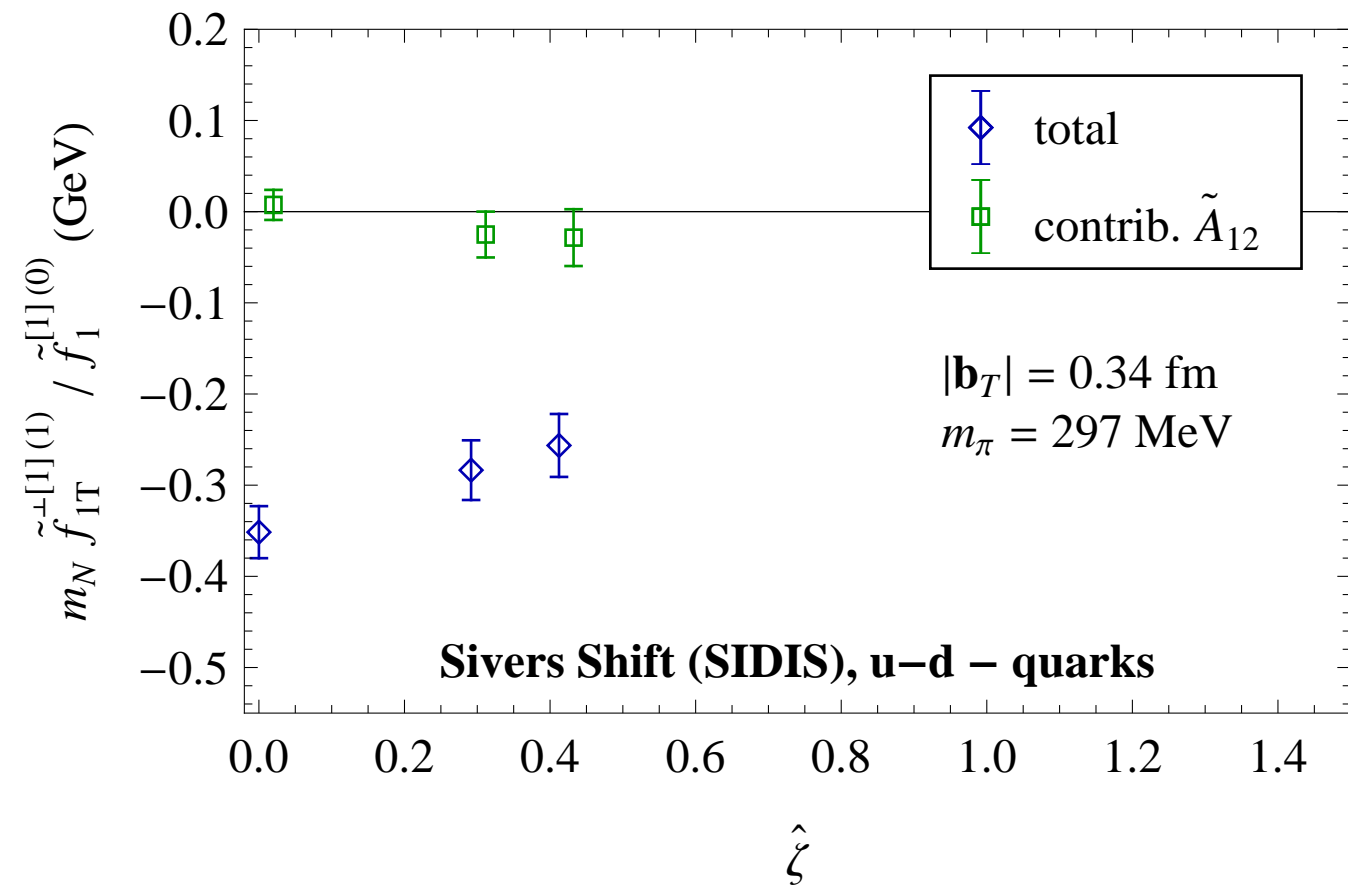
Results: Sivers shift

Dependence of SIDIS limit on $|b_T|$



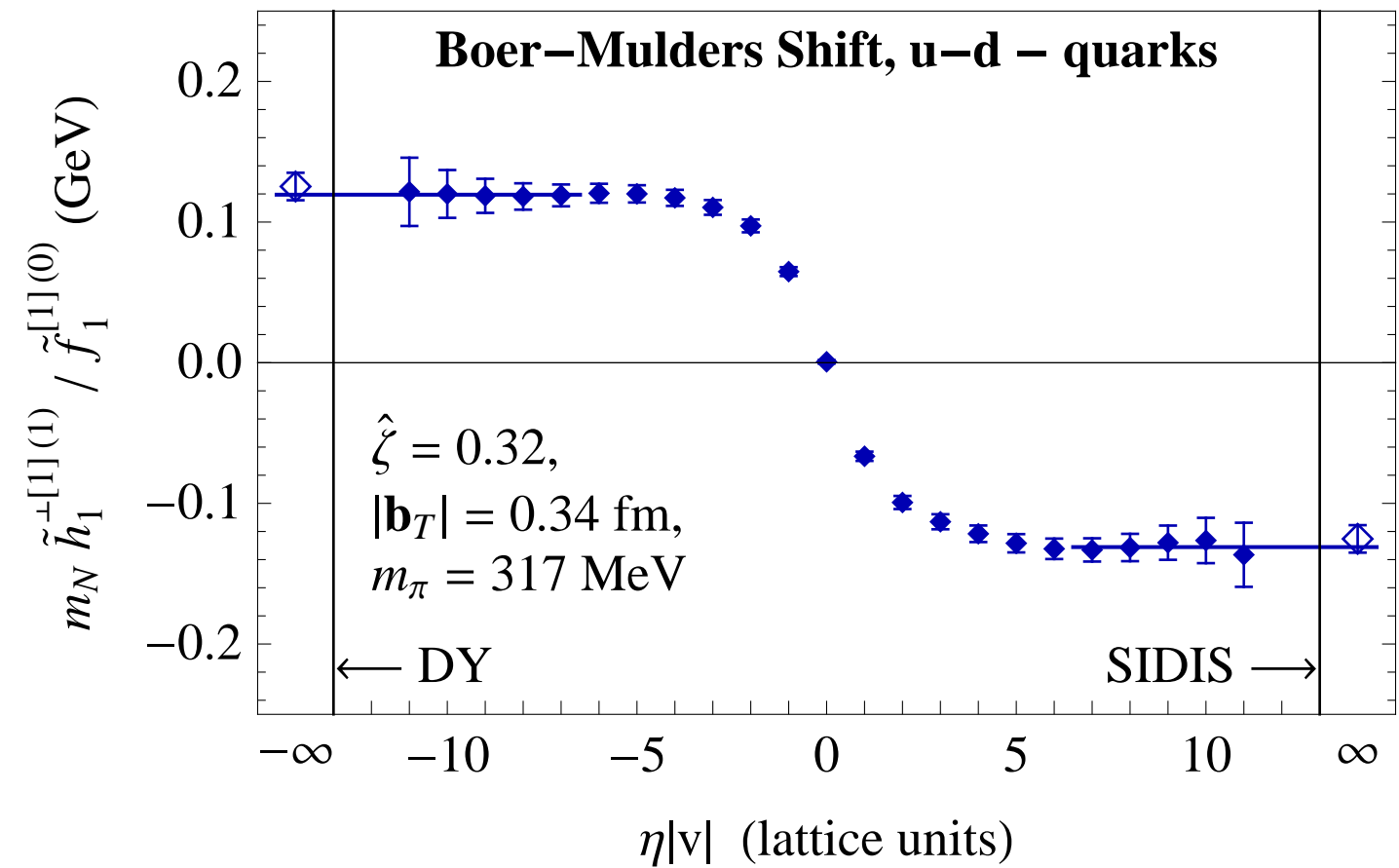
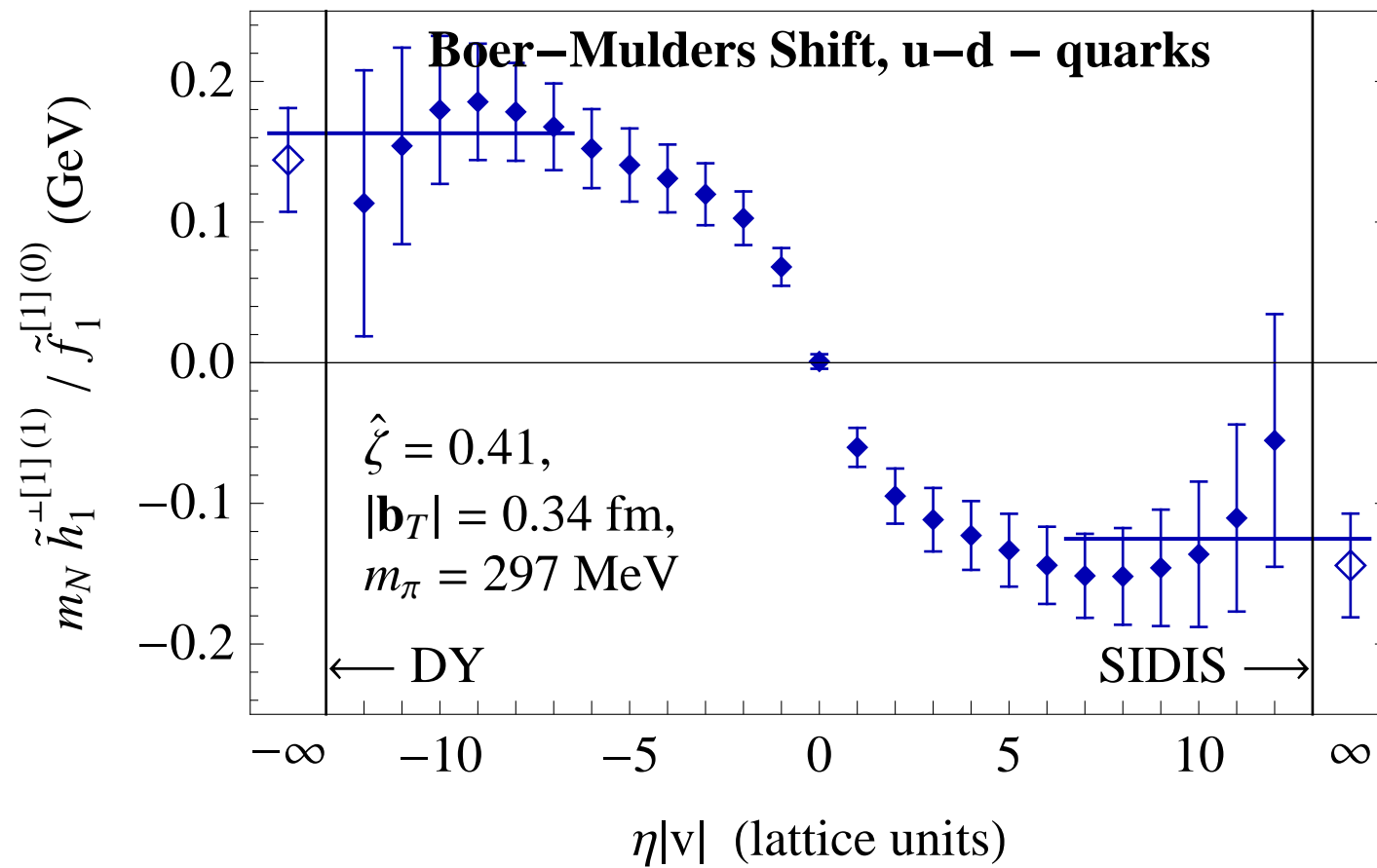
Results: Sivers shift

Dependence of SIDIS limit on $\hat{\zeta}$



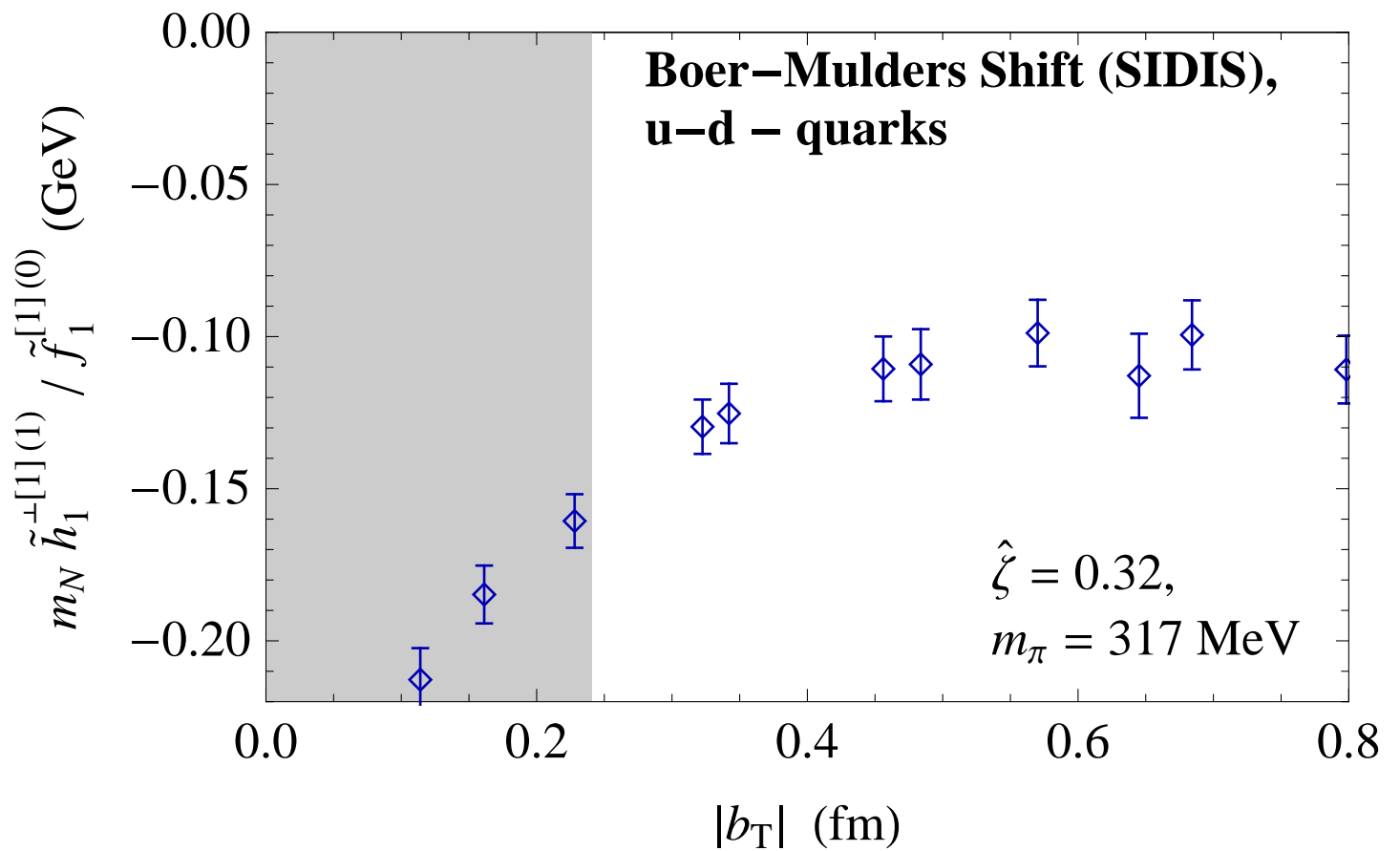
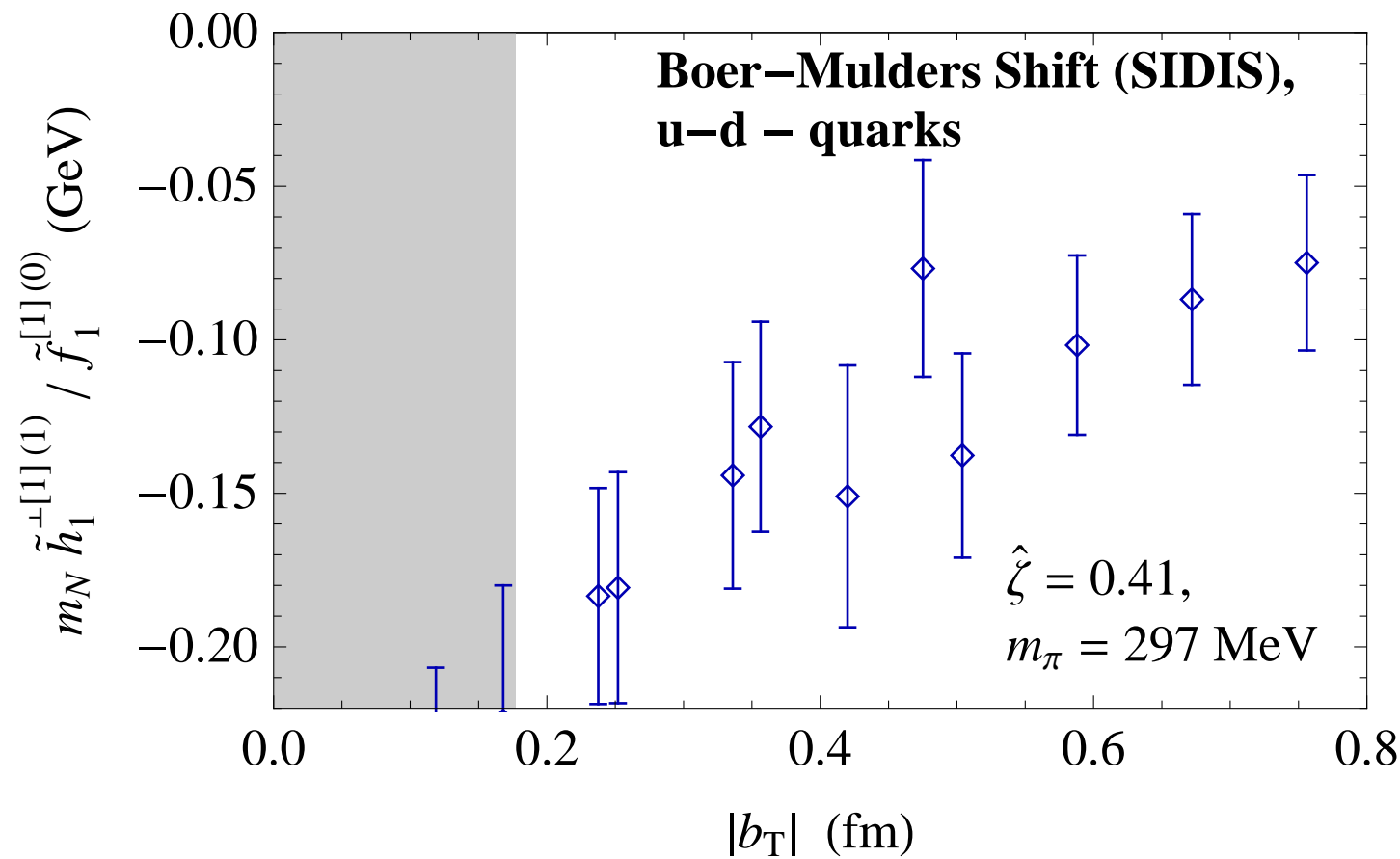
Results: Boer-Mulders shift

Dependence on staple extent



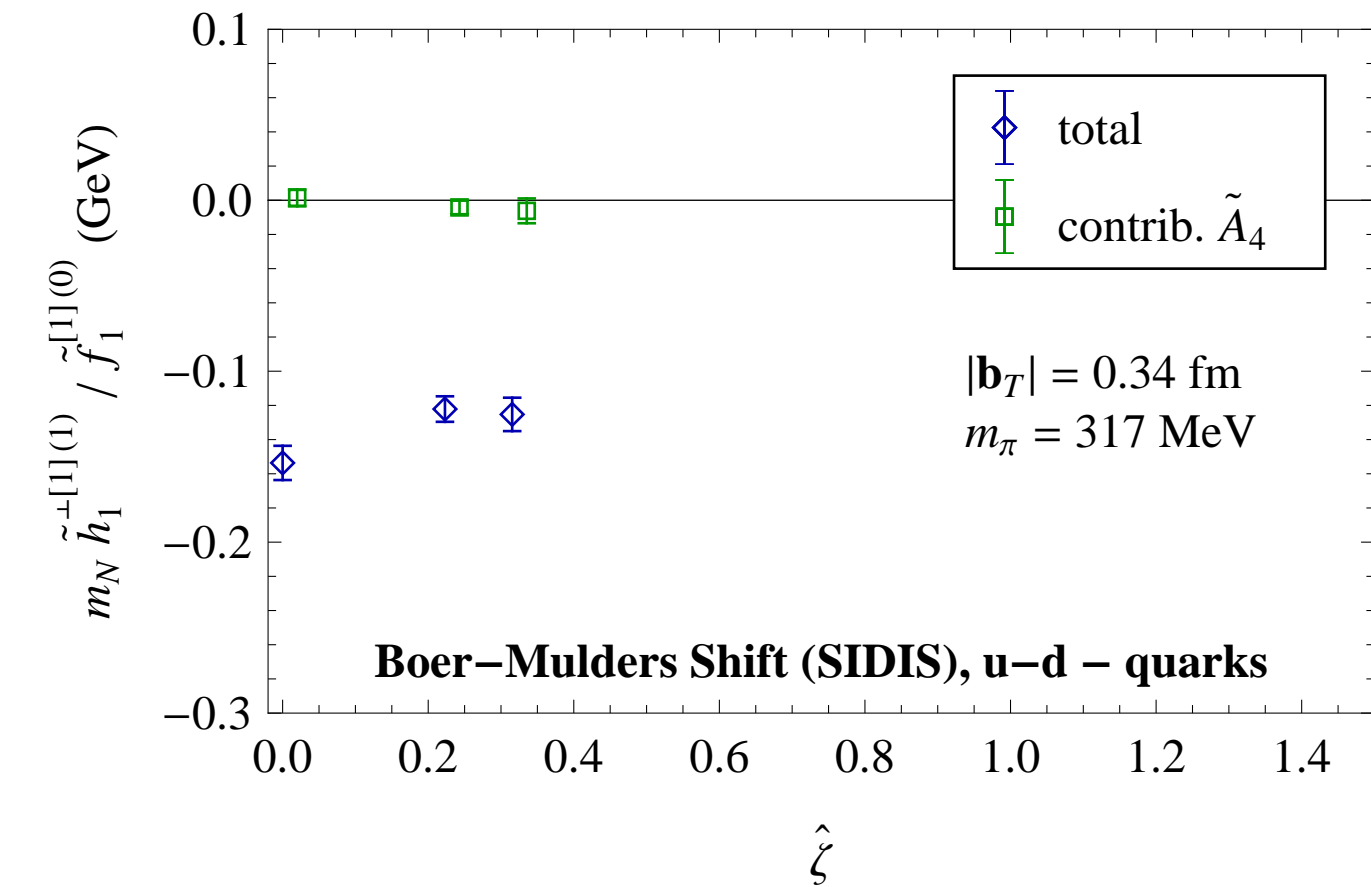
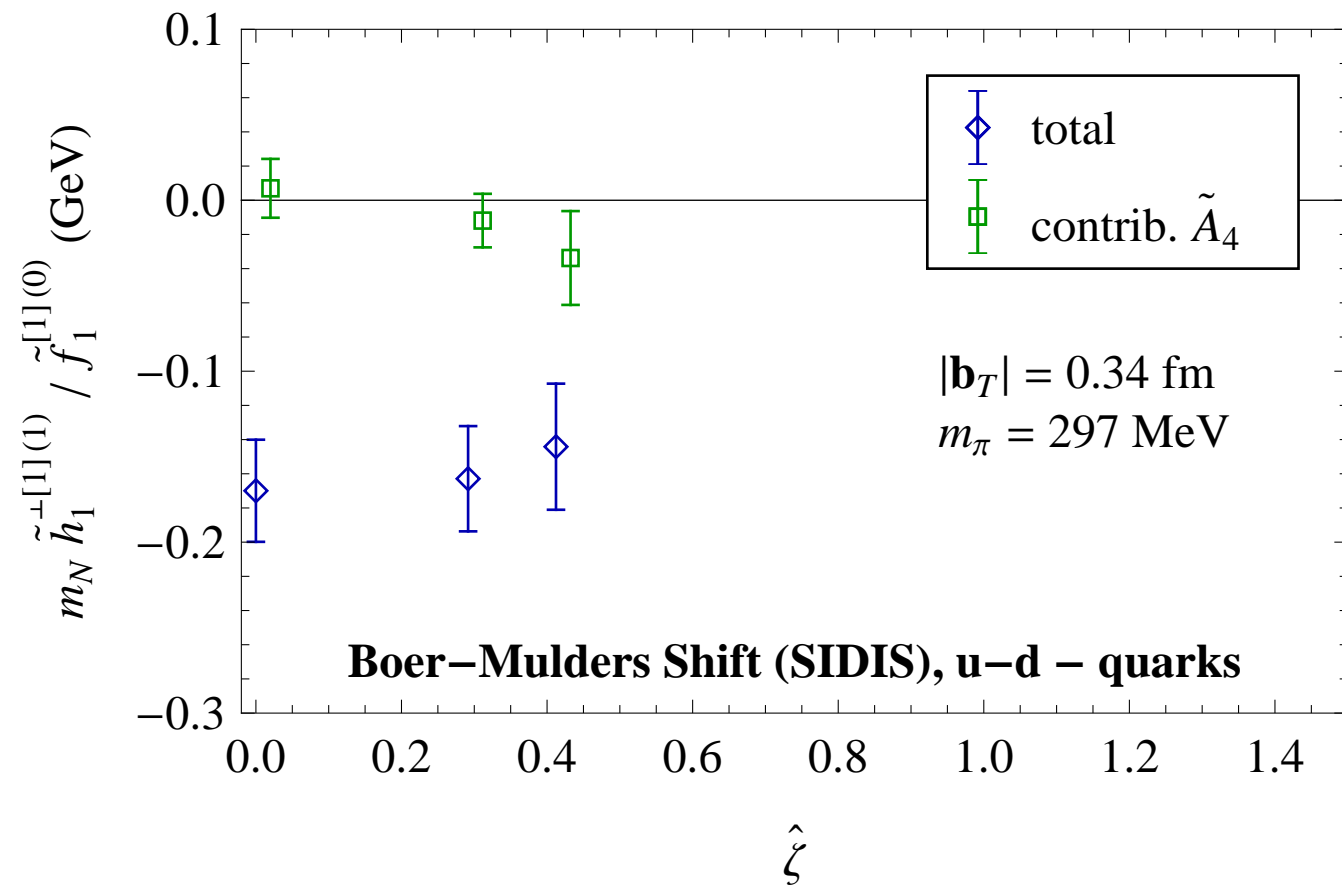
Results: Boer-Mulders shift

Dependence of SIDIS limit on $|b_T|$



Results: Boer-Mulders shift

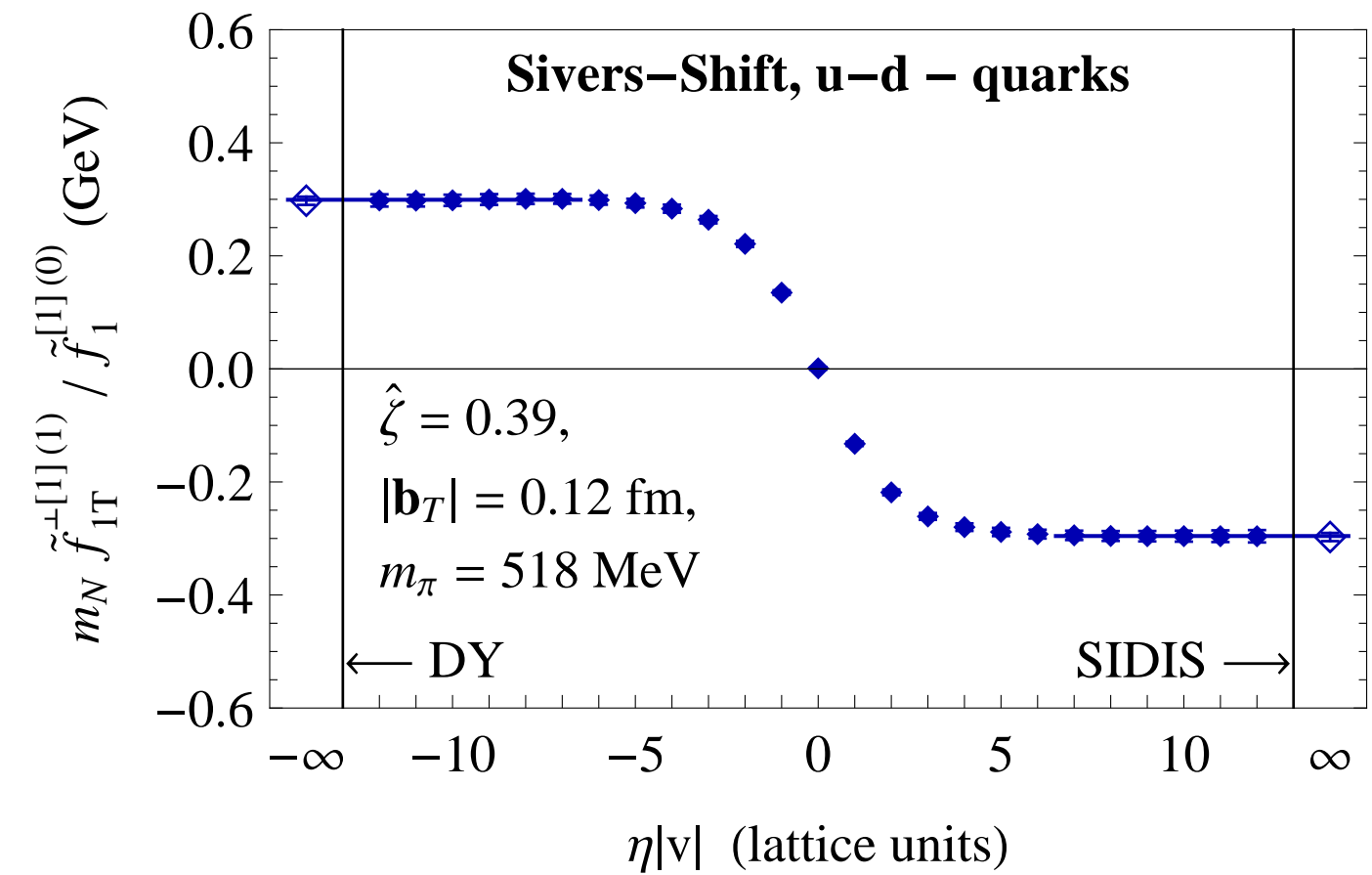
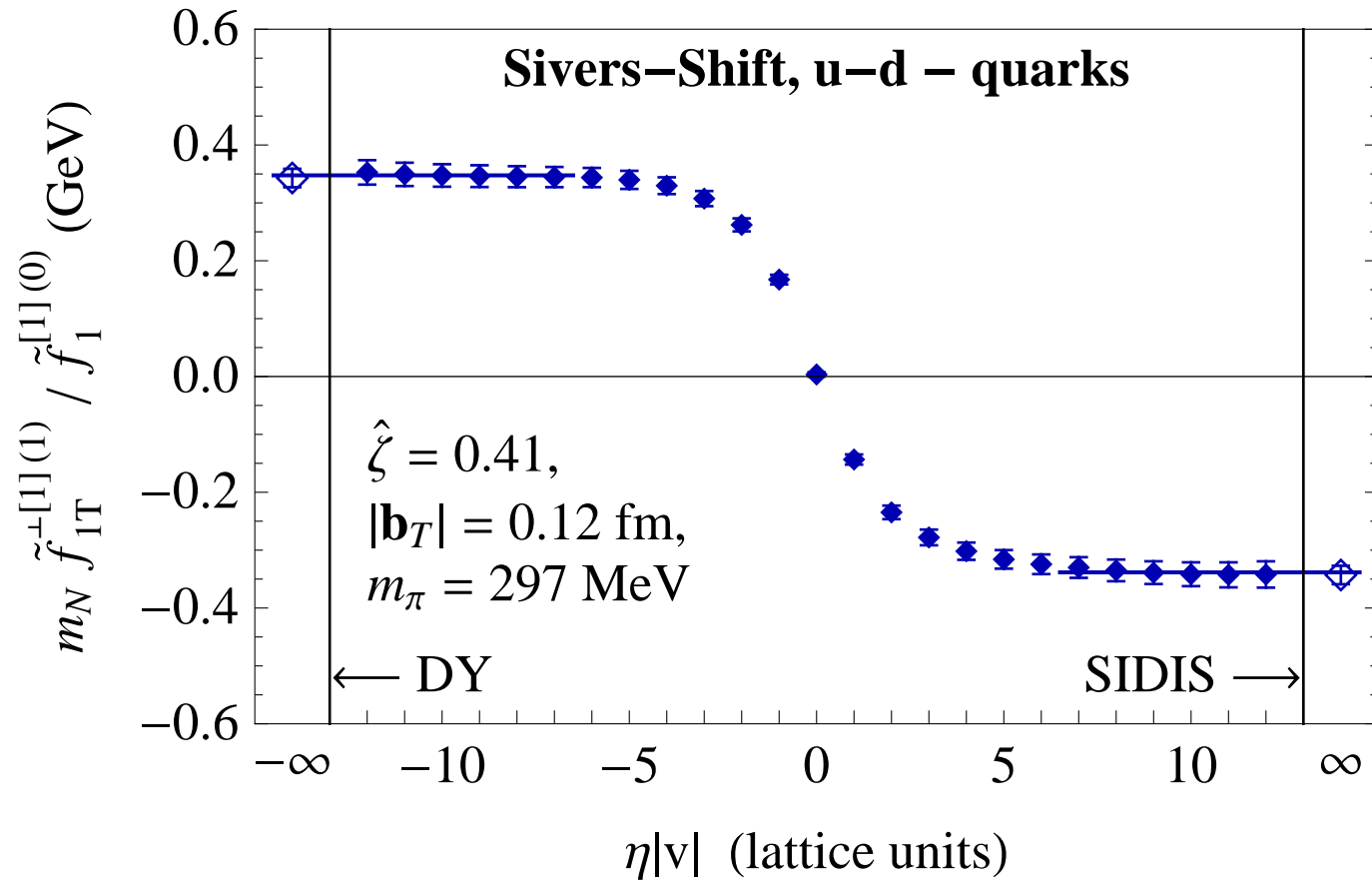
Dependence of SIDIS limit on $\hat{\zeta}$



Dependence on the pion mass

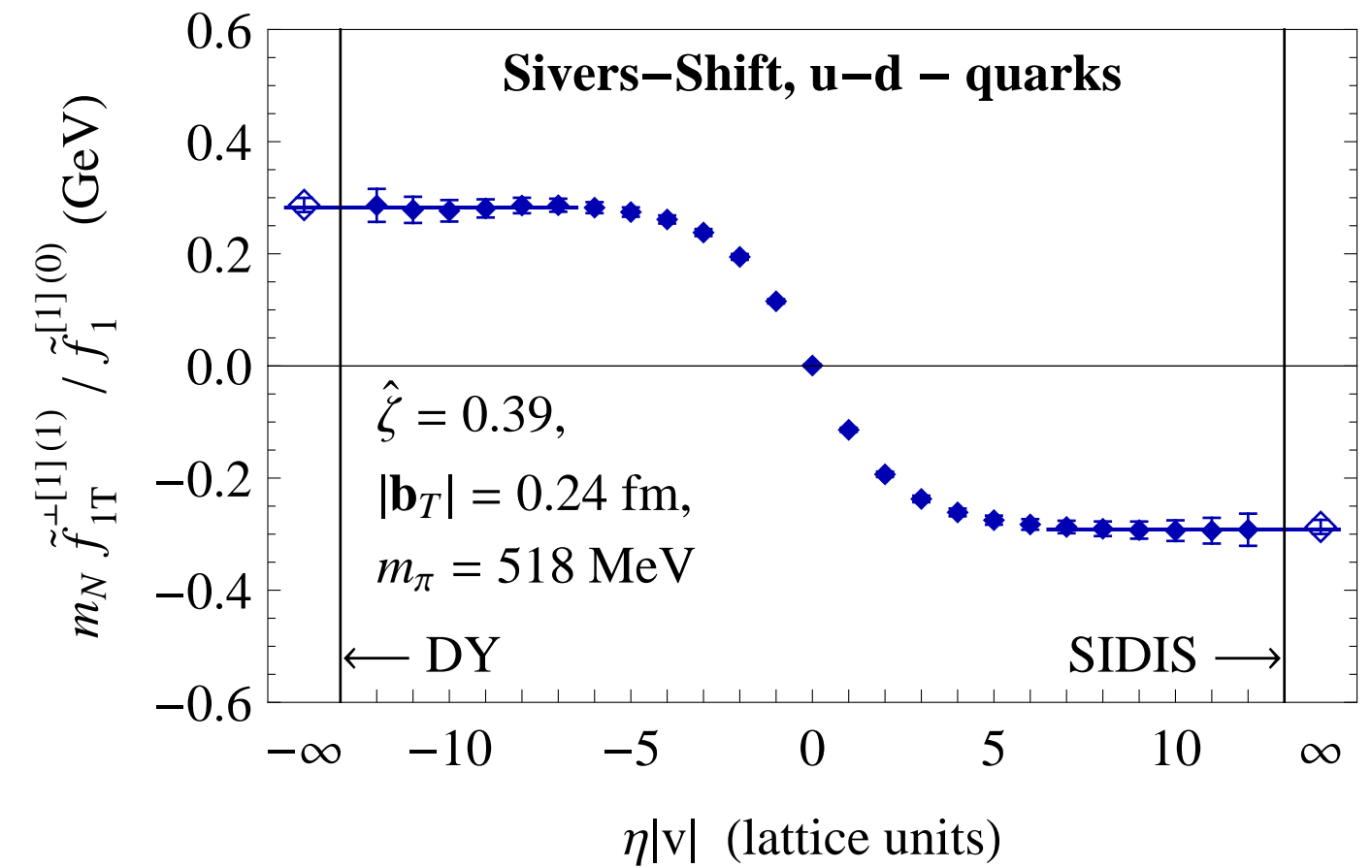
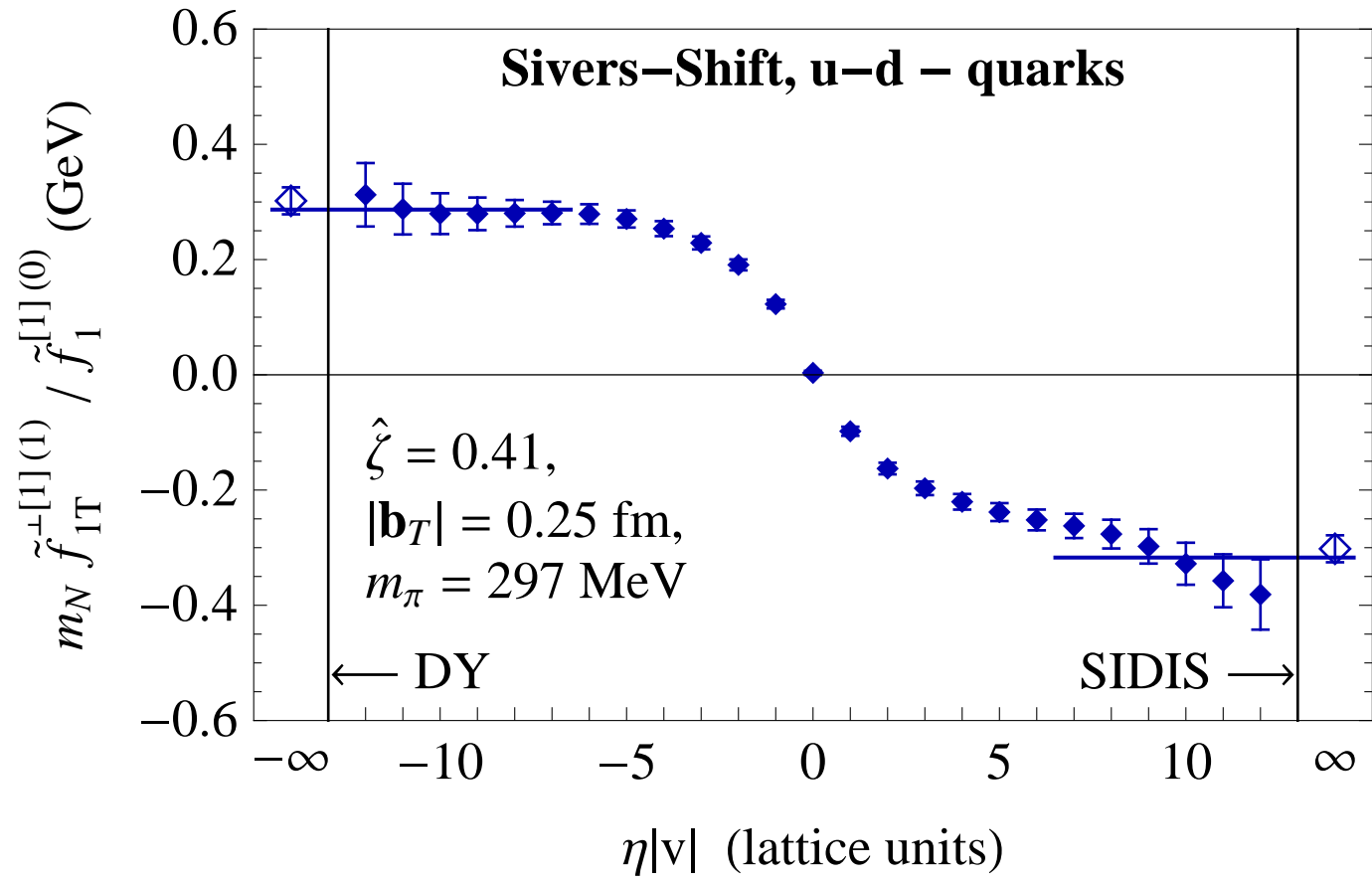
Results: Sivers shift

Dependence on staple extent; sequence of panels at different $|b_T|$



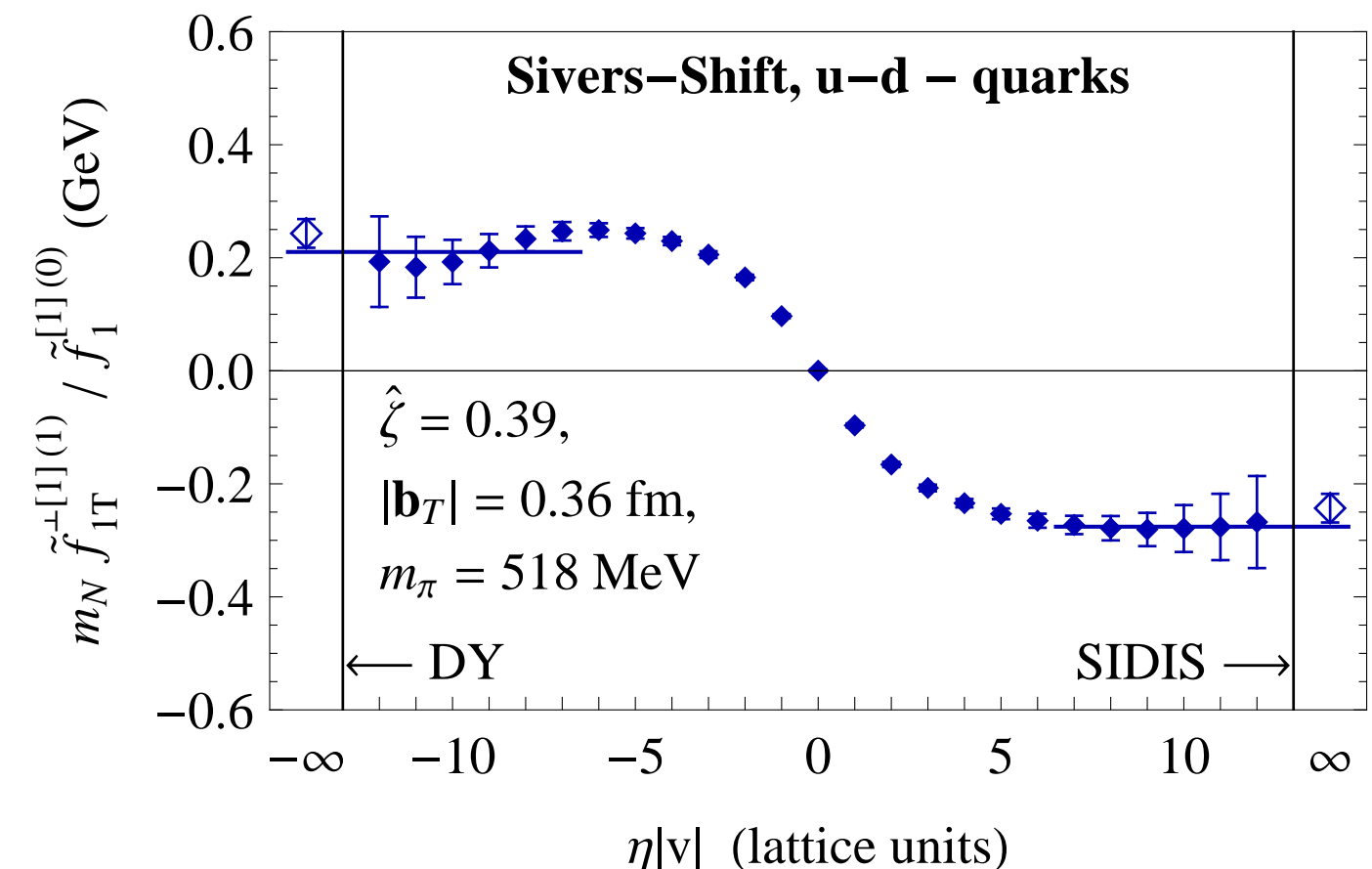
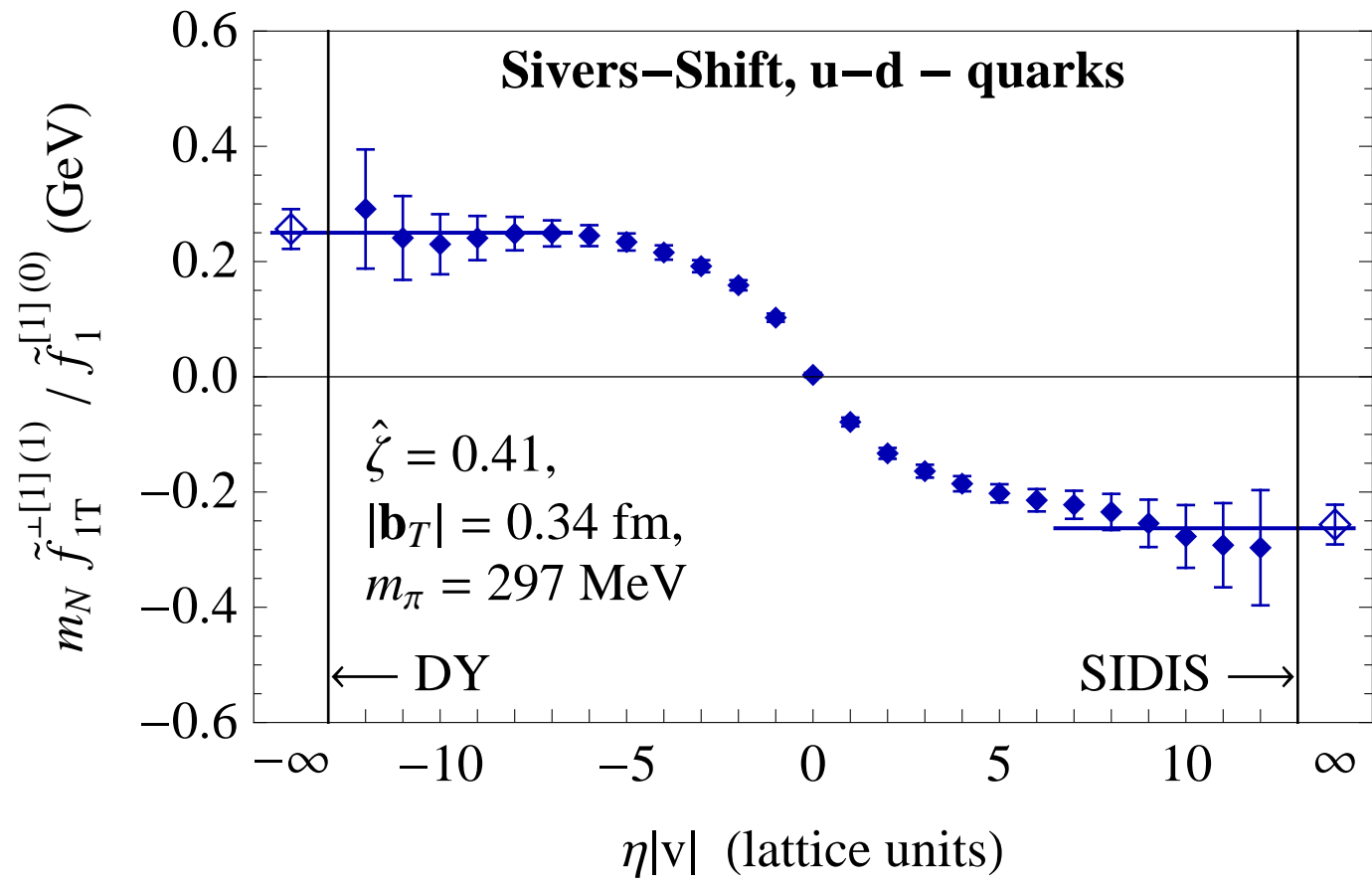
Results: Sivers shift

Dependence on staple extent; sequence of panels at different $|b_T|$



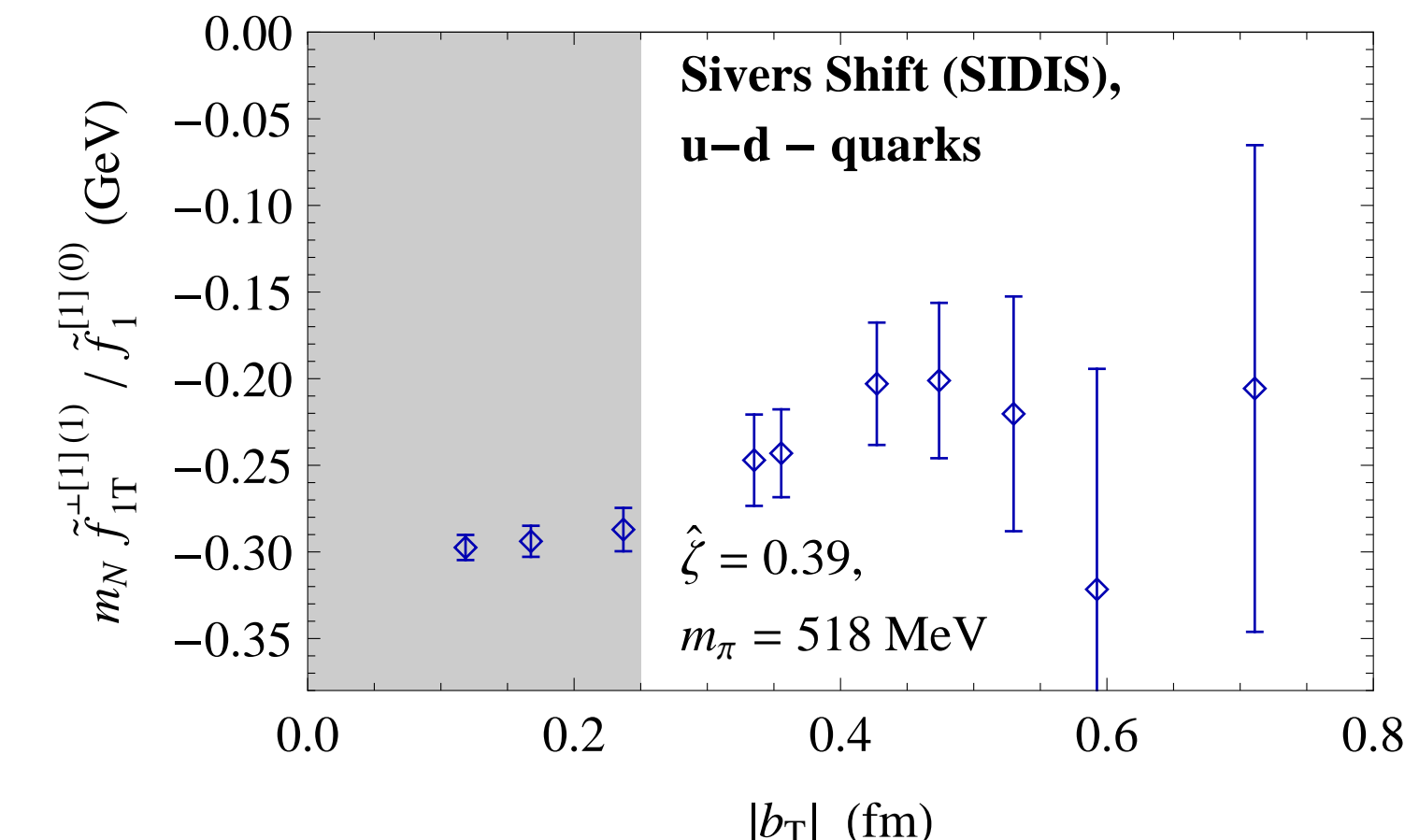
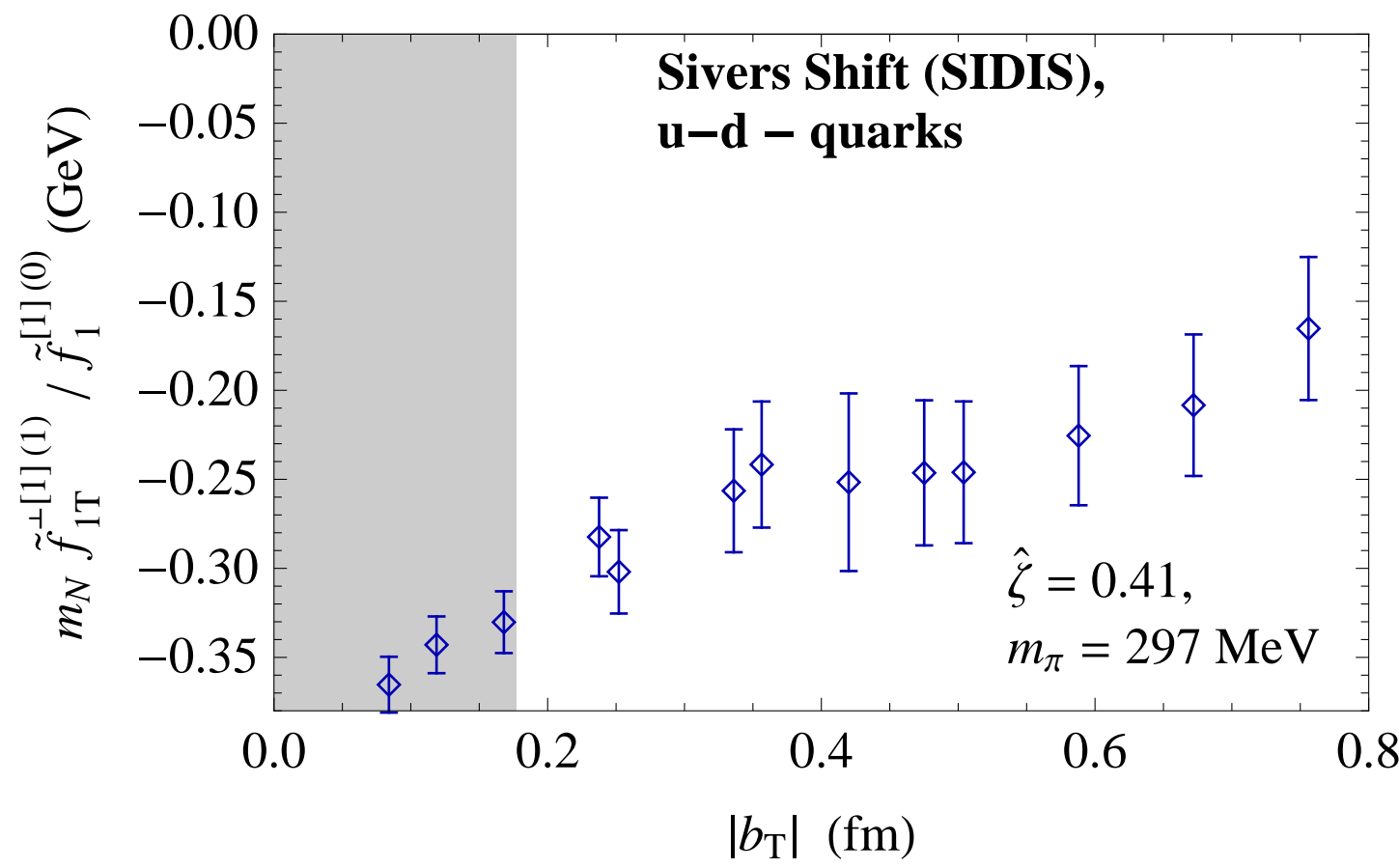
Results: Sivers shift

Dependence on staple extent; sequence of panels at different $|b_T|$



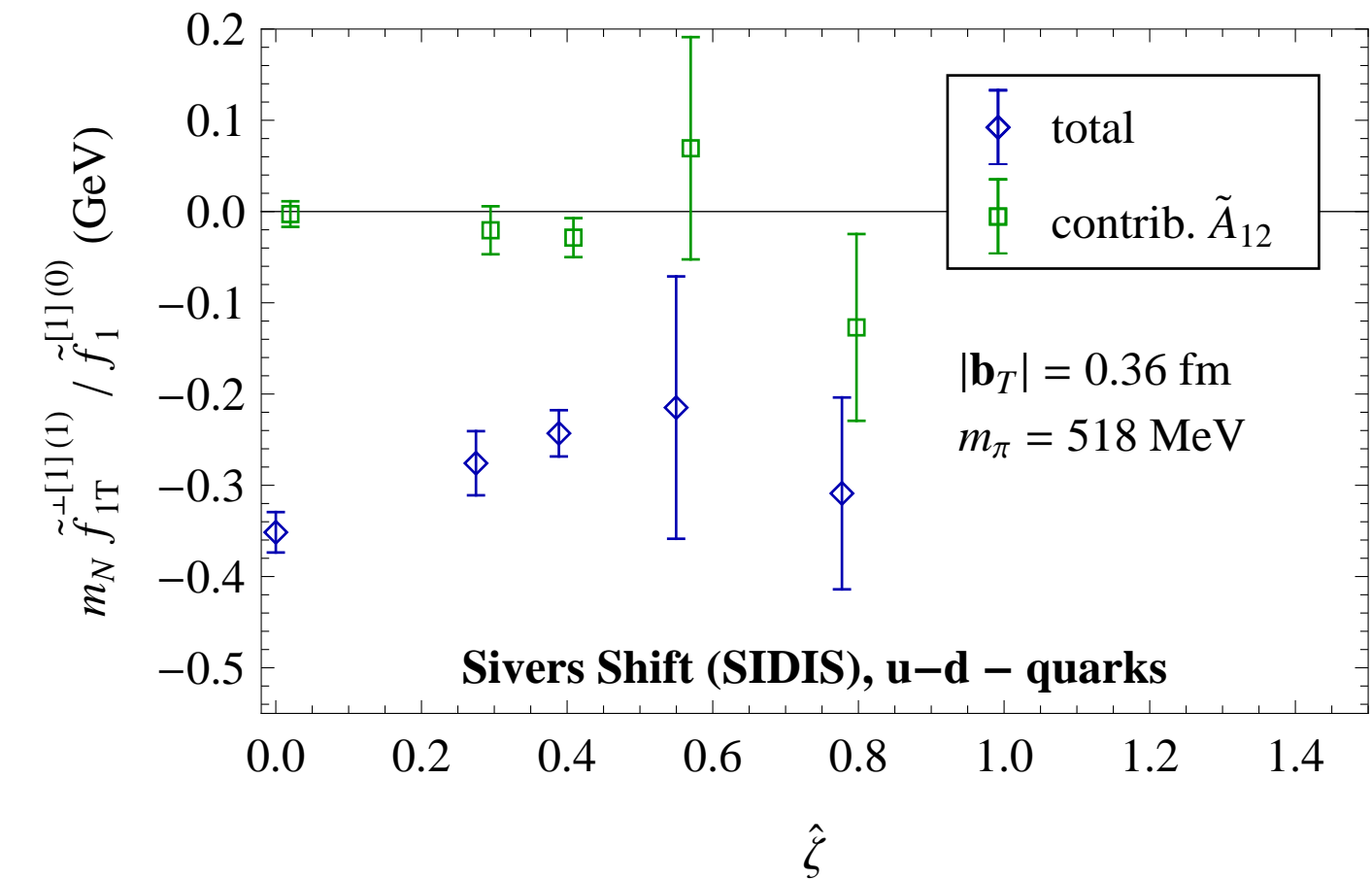
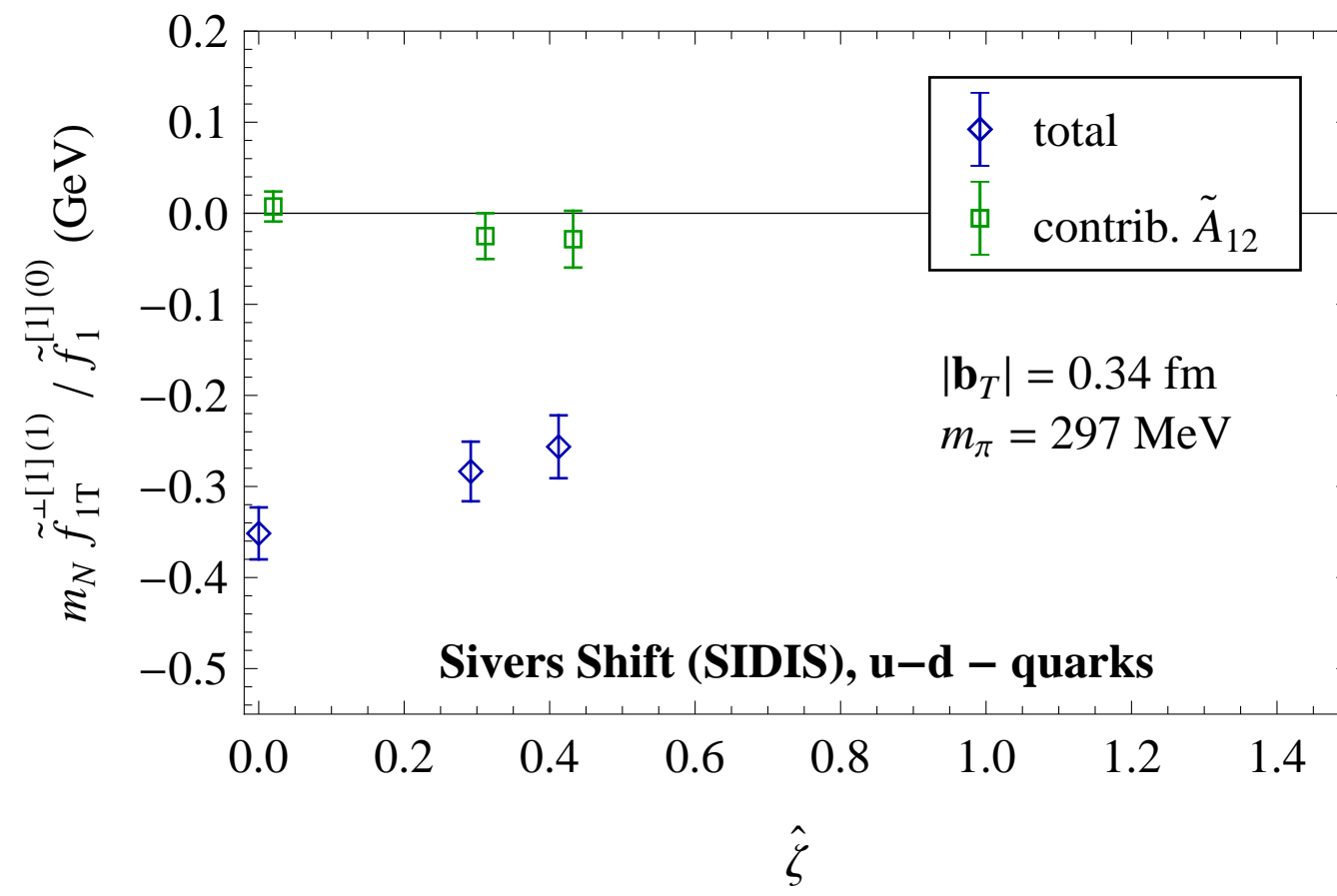
Results: Sivers shift

Dependence of SIDIS limit on $|b_T|$



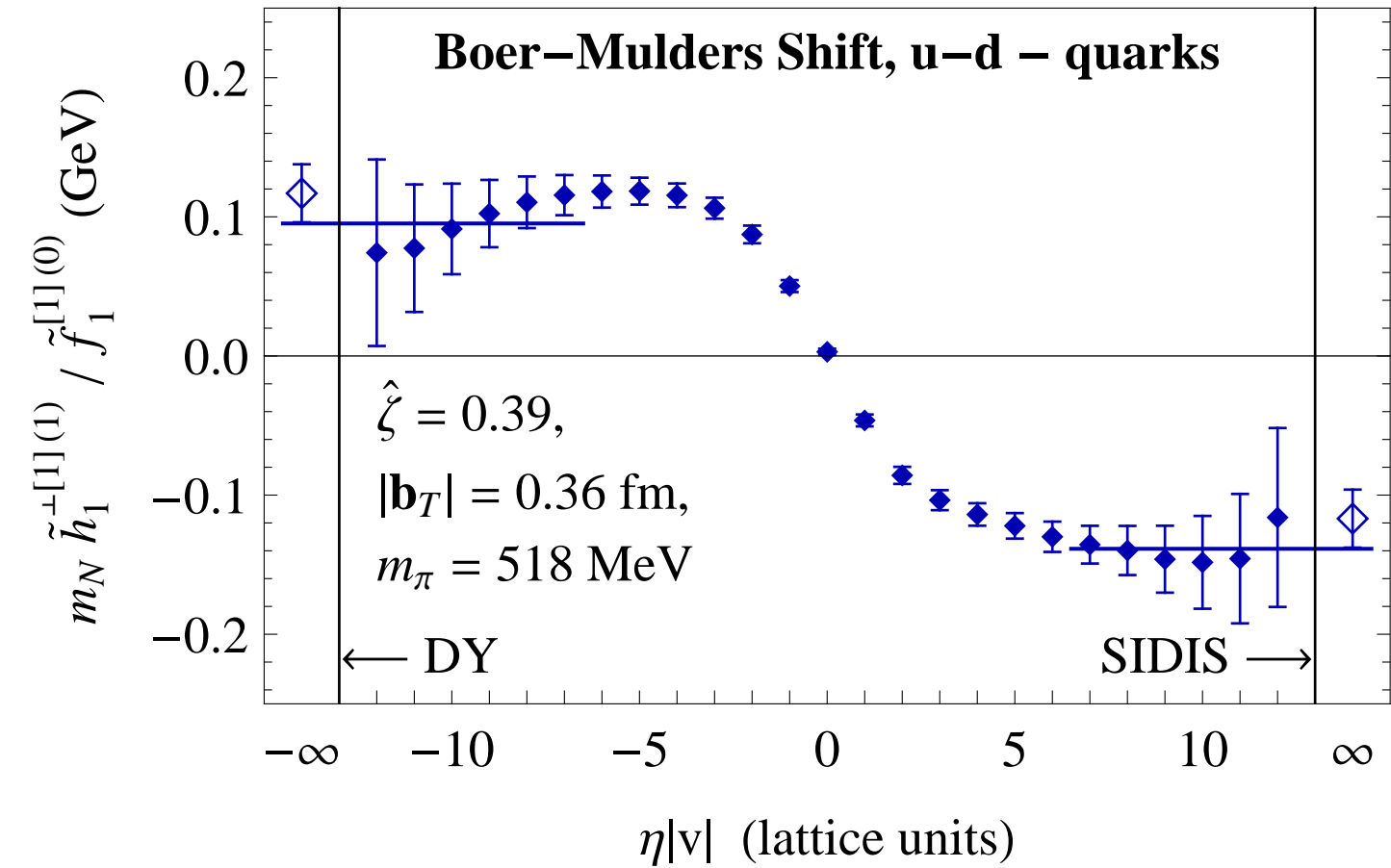
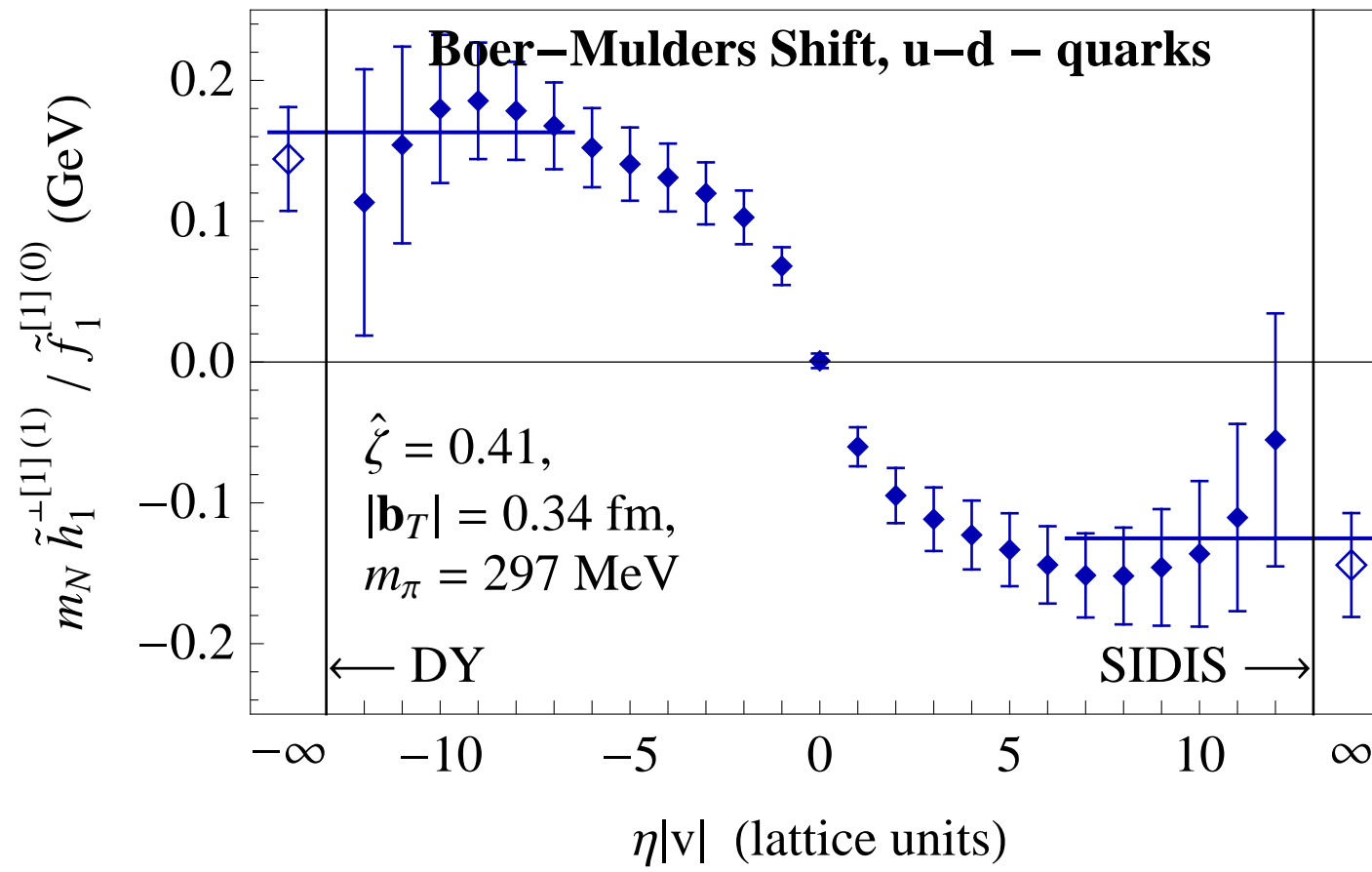
Results: Sivers shift

Dependence of SIDIS limit on $\hat{\zeta}$



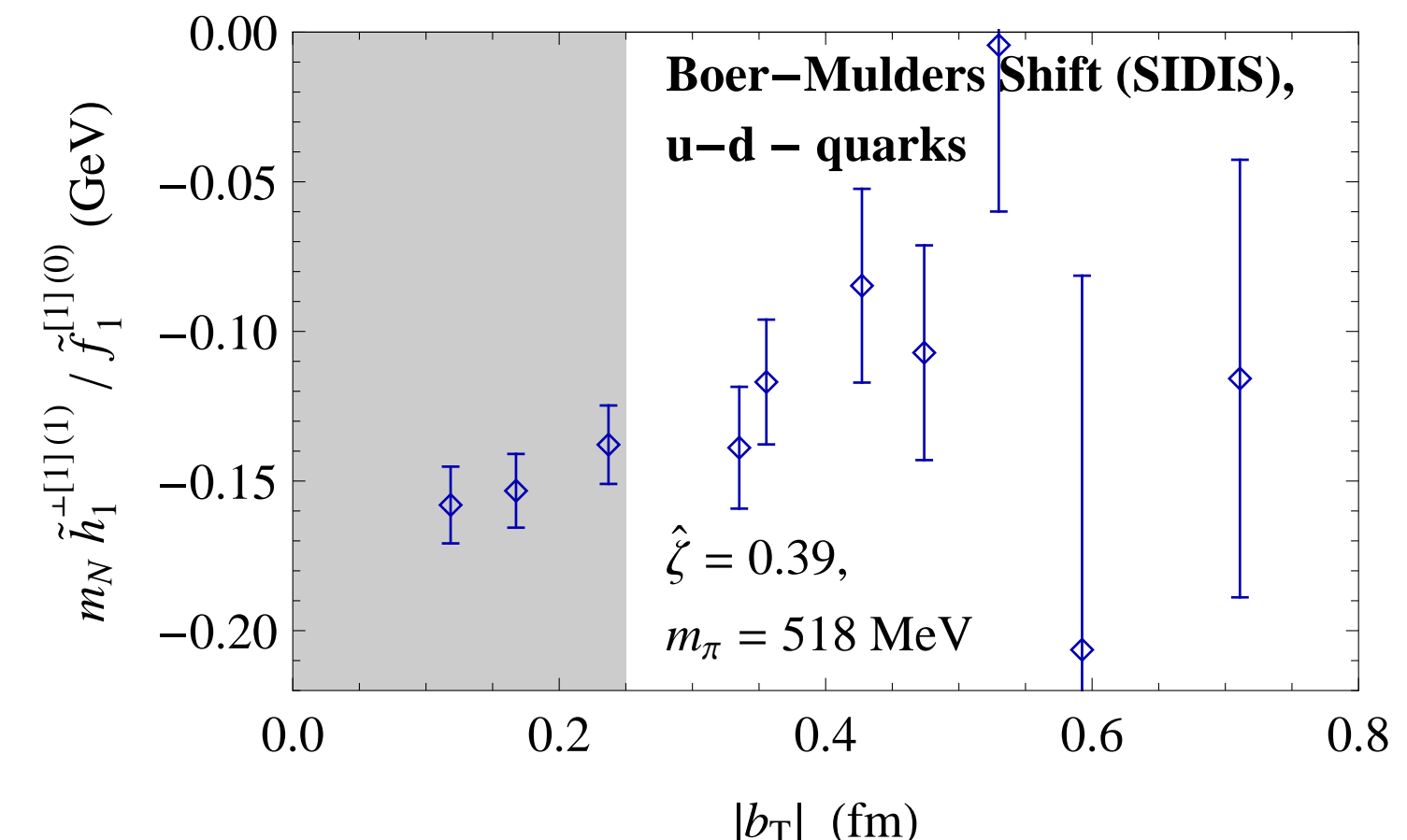
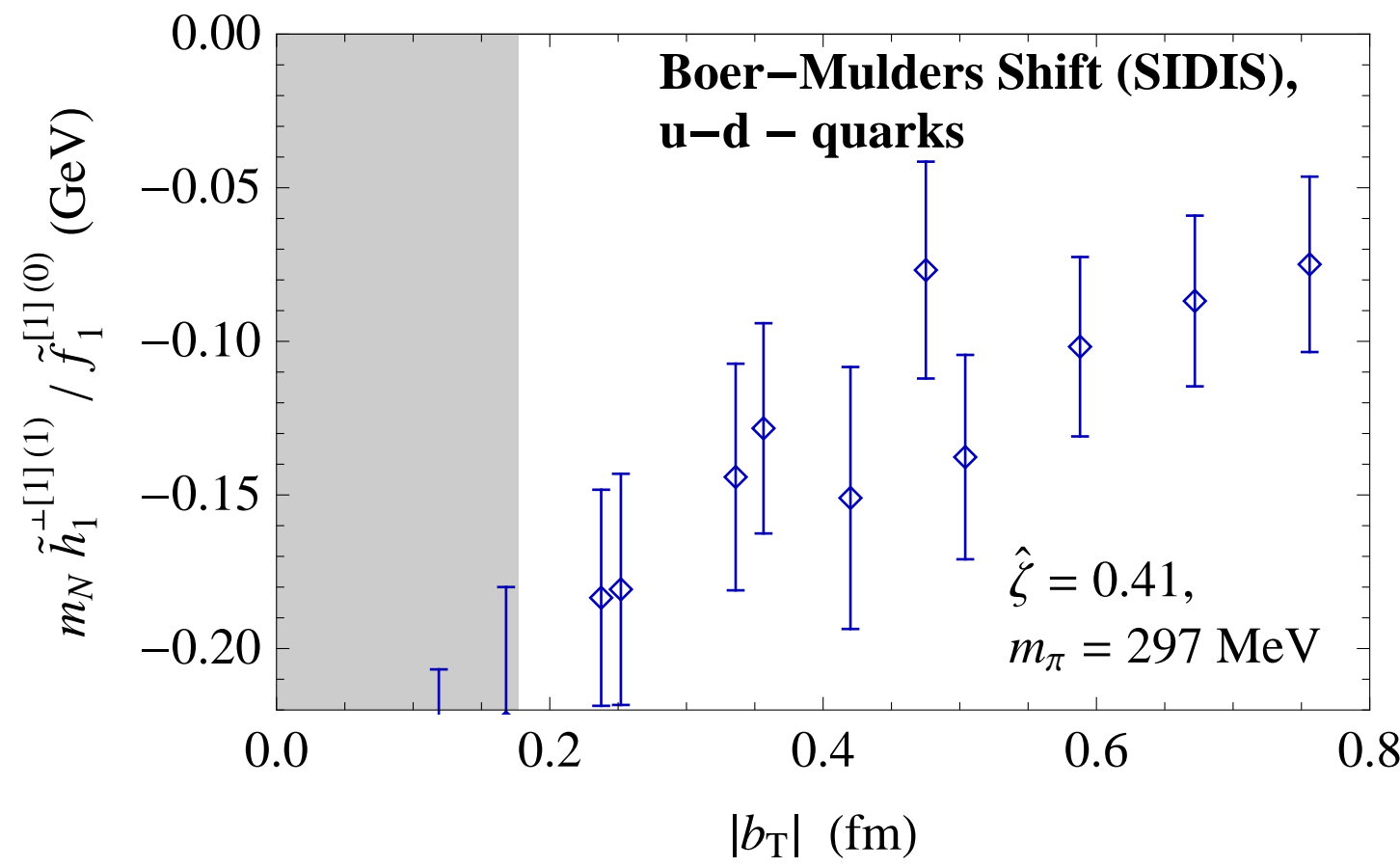
Results: Boer-Mulders shift

Dependence on staple extent



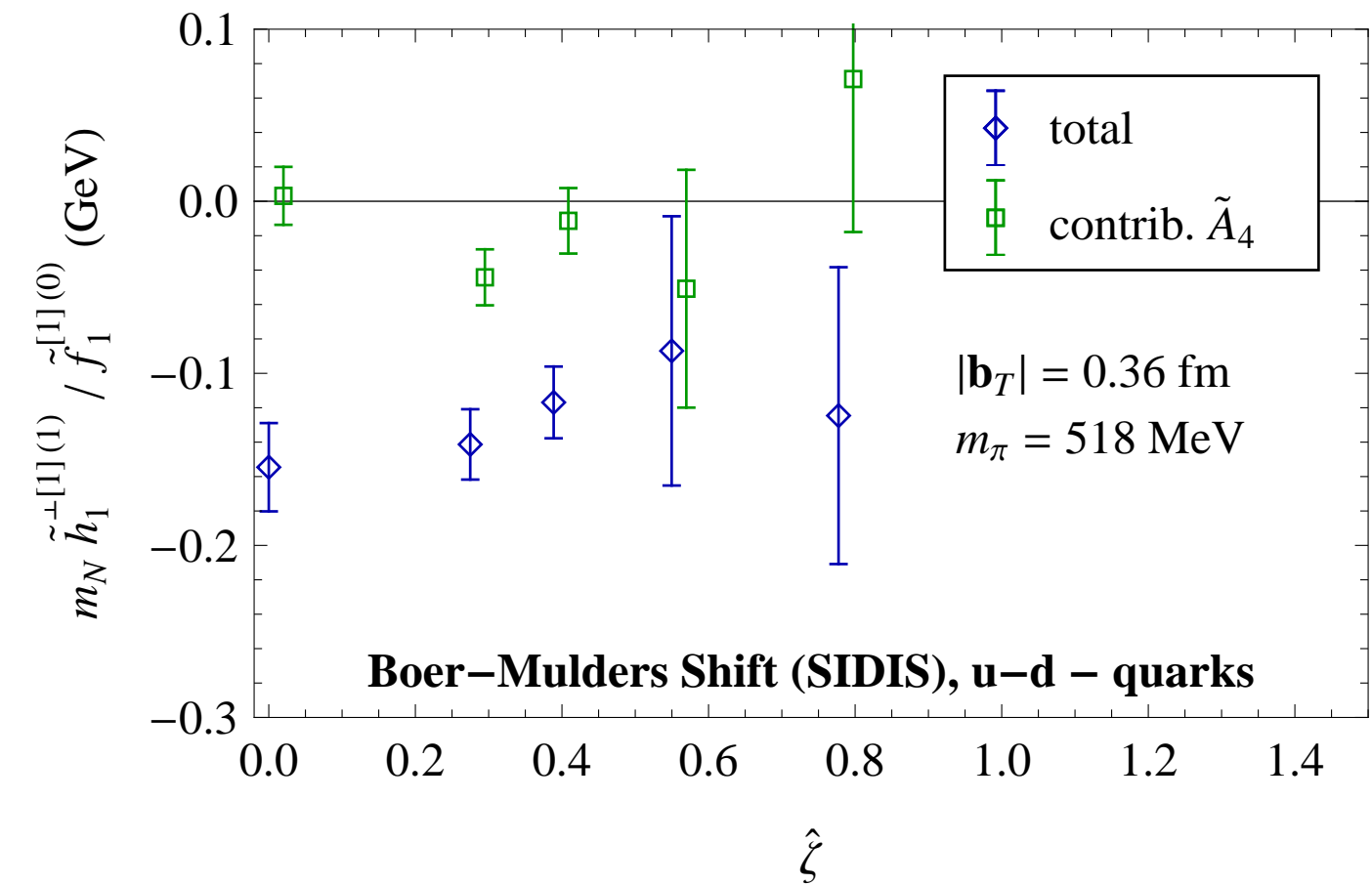
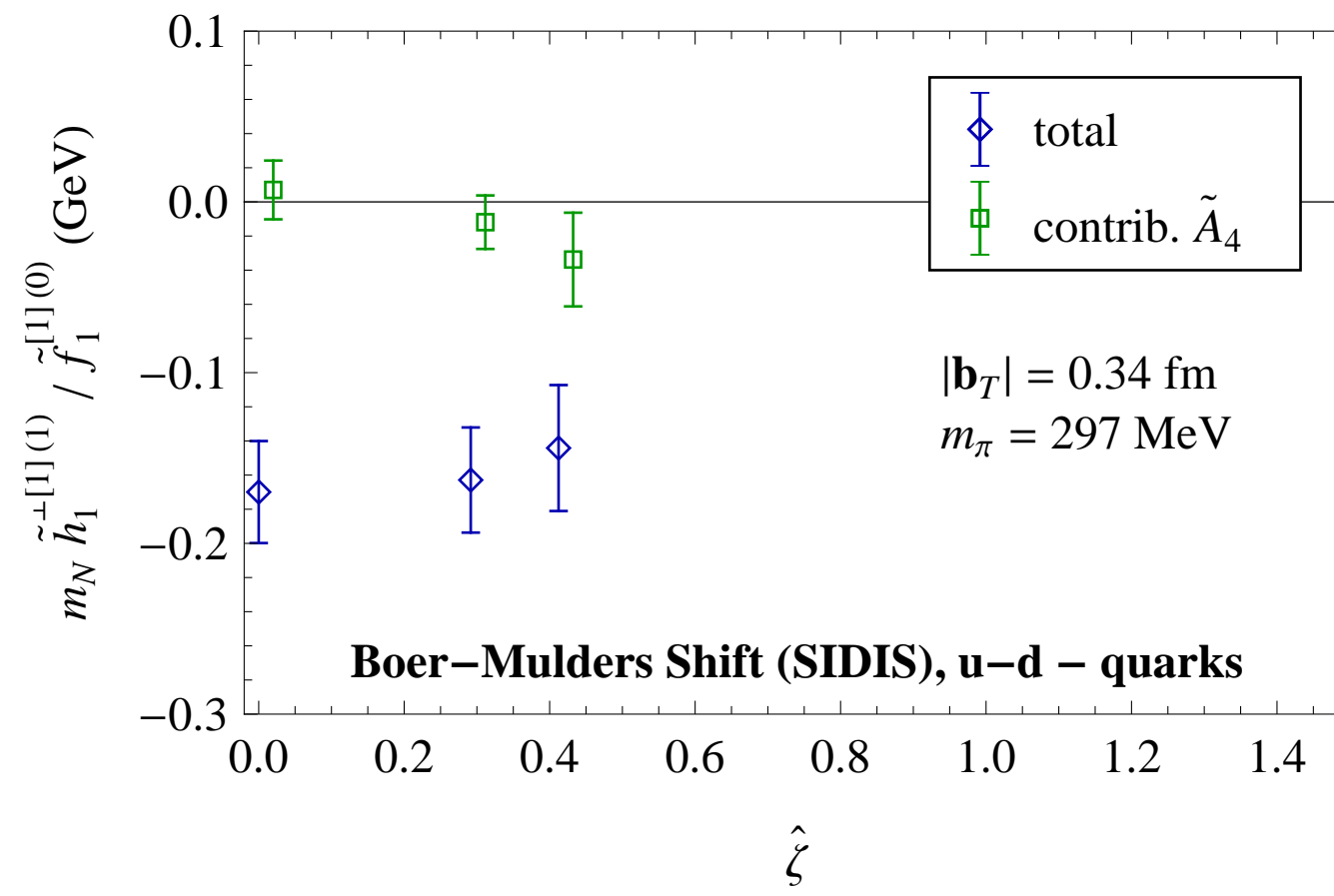
Results: Boer-Mulders shift

Dependence of SIDIS limit on $|b_T|$



Results: Boer-Mulders shift

Dependence of SIDIS limit on $\hat{\zeta}$



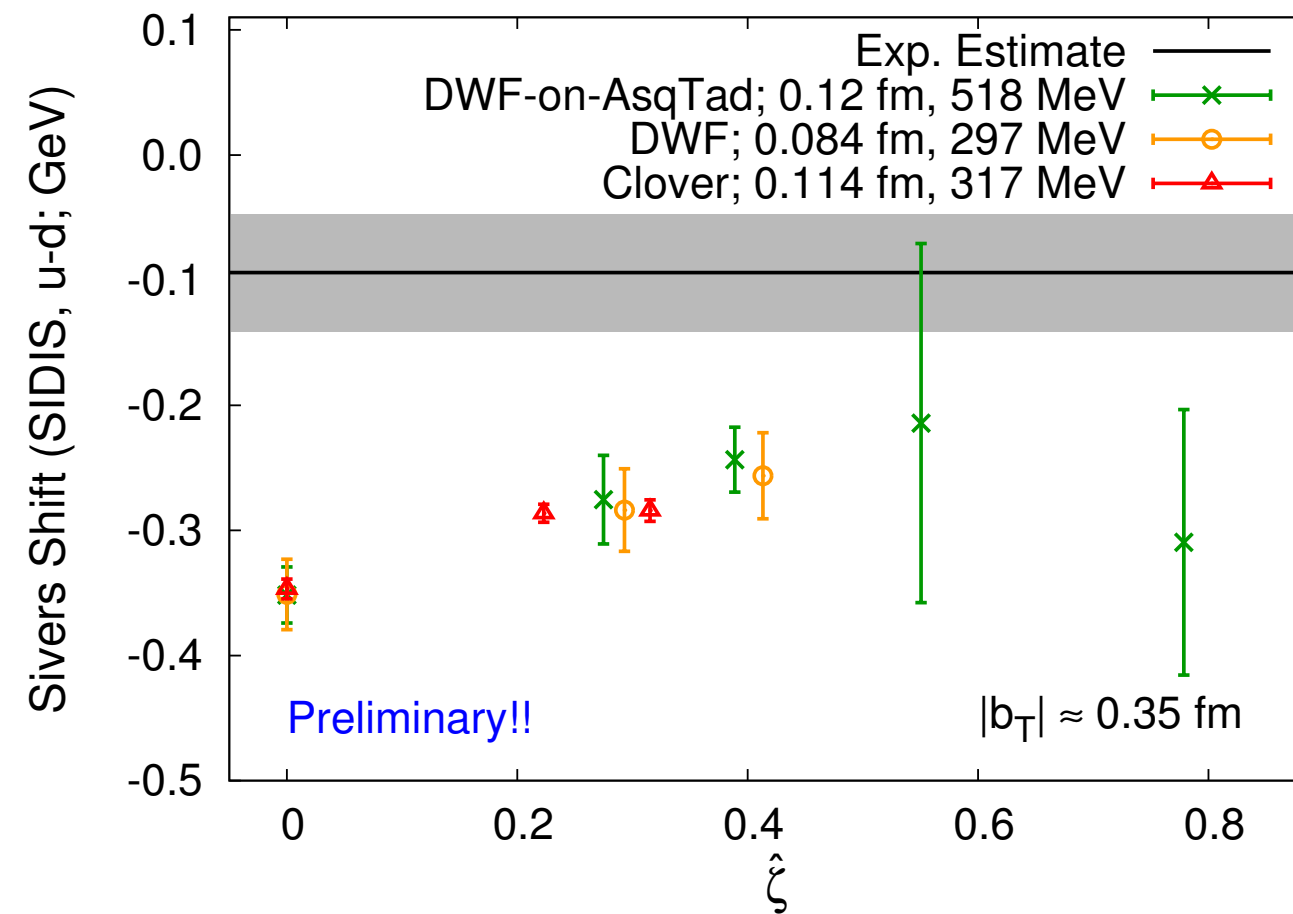
Progressing toward the physical pion mass

Currently in production: RBC/UKQCD DWF ensemble at 180 MeV pion mass (to be completed this year)

2015 production: RBC/UKQCD DWF ensemble at the physical pion mass

Results: Sivers shift summary

Dependence of SIDIS limit on $\hat{\zeta}$



Experimental value from global fit to HERMES, COMPASS and JLab data,
M. Echevarria, A. Idilbi, Z.-B. Kang and I. Vitev, Phys. Rev. D 89 (2014) 074013

Conclusions and Outlook

- Continued exploration of TMDs using bilocal quark operators with staple-shaped gauge link structures; exploration of challenges posed by $\hat{\zeta} \rightarrow \infty$ limit, discretization effects, physical limit.
- To avoid soft factors, multiplicative renormalization constants, considered appropriate ratios of Fourier-transformed TMDs (“shifts”).
- These observables show no statistically significant variation under the considered changes of action, lattice spacing and pion mass, except at very short distances.
- Production underway on an RBC/UKQCD 180 MeV pion mass ensemble, production on an RBC/UKQCD ensemble at physical pion mass in preparation.
- Generalization to mixed transverse momentum / transverse position observables (Wigner functions) underway, to directly access quark orbital angular momentum.

Relation to Ji Large Momentum Effective Theory (LaMET)

Phenomenology

Lattice QCD

